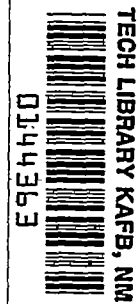


NACA RM L52D18



NACA

RESEARCH MEMORANDUM

WIND-TUNNEL INVESTIGATION OF THE AERODYNAMIC
CHARACTERISTICS IN PITCH OF WING-FUSELAGE
COMBINATIONS AT HIGH-SUBSONIC SPEEDS

SWEEP SERIES

By James W. Wiggins and Richard E. Kuhn

Langley Aeronautical Laboratory
Langley Field, Va.

CLASSIFIED DOCUMENT

NATIONAL ADVISORY COMMITTEE
FOR AERONAUTICS

WASHINGTON

July 2, 1952

*Receipt signature
required*

Classification cancelled (or changed to) Unclassified
By Authority Nasa Tech Pub Announcement #99
(OFFICER AUTHORIZED TO CHANGE)

By NK 13 Apr 56

GRADE OF OFFICER MAKING CHANGE) NK

6 Apr 61
DATE



NATIONAL ADVISORY COMMITTEE FOR AERONAUTICS

RESEARCH MEMORANDUM

WIND-TUNNEL INVESTIGATION OF THE AERODYNAMIC
CHARACTERISTICS IN PITCH OF WING-FUSELAGE
COMBINATIONS AT HIGH-SUBSONIC SPEEDS

SWEEP SERIES

By James W. Wiggins and Richard E. Kuhn

SUMMARY

The results presented in the present paper are a part of a program conducted to investigate the aerodynamic characteristics in pitch, yaw, and steady roll of various model configurations with variations in the wing geometric parameters. This paper presents the aerodynamic characteristics in pitch of wing-fuselage combinations with wings of aspect ratio 4, taper ratio of 0.6 and sweep angles varying from 3.6° to 60° . The Mach number range was from 0.40 to approximately 0.95 and the Reynolds number ranged from 2,000,000 to 3,500,000. Inasmuch as results of pitch tests on many of the wing plan forms being used in this program have been reported previously, the data of the present investigation are presented primarily to provide a consistent basis for the interpretation of results from phases of the program that deal with characteristics in yaw and in steady roll.

The increase of lift-curve slope with Mach number and the decrease with sweep predicted by available theory are in fair agreement with the experimental data. The experimental wing-fuselage aerodynamic center showed little variation with Mach number up to the force-break Mach number. Above this point all wings exhibited a rapid rearward movement of the aerodynamic center. An increase in the sweep angle increased the drag-rise Mach number and, in general, increased the drag due to lift. The wings with higher sweepback showed no change in drag due to lift over the test Mach number range. The maximum lift-drag ratios decreased with increasing sweep and were only slightly affected by Mach number below the drag-rise Mach number. Above the drag-rise Mach number all wings showed a rapid decrease in maximum lift-drag ratio.

INTRODUCTION

A systematic research program is being conducted in the Langley high-speed 7- by 10-foot wind tunnel to determine the aerodynamic characteristics of various model configurations in pitch and yaw and during steady rolling up to a Mach number of about 0.95. The Reynolds number range for the sting-supported models varies from 1,500,000 to 6,000,000, depending on the wing plan form and test Mach number.

The wing plan forms used in the current research program are similar, in general, to the plan forms investigated at lower Reynolds numbers during a previous research program which utilized the transonic-bump technique for obtaining results at transonic speeds. Some of the results obtained from the transonic-bump program have been summarized in reference 1. Some similar or related wing plan forms also have been investigated in other facilities (refs. 2 to 5). A comparison of aerodynamic characteristics in pitch as obtained by different test techniques has been reported in reference 6. The effects of aspect ratio on the pitch characteristics of 45° swept wings of 0.6 taper ratio and an NACA 65A006 airfoil section are presented in reference 7.

The present paper presents results of an investigation of the effects of sweep on the aerodynamic characteristics in pitch of wings of aspect ratio 4, taper ratio 0.6, and with an NACA 65A006 airfoil section in combination with a common fuselage. Since somewhat similar investigations already have been reported, the present paper is intended primarily to provide a consistent basis for the interpretation of results from phases of this program that deal with characteristics in yaw and in steady, roll.

COEFFICIENTS AND SYMBOLS

The symbols used in the present paper are defined in the following list. All forces and moments are presented relative to the quarter chord of the mean aerodynamic chord.

C_L	lift coefficient, $Lift/qS$
C_D	drag coefficient, $Drag/qS$
C_m	pitching-moment coefficient, $Pitching\ moment/qS\bar{c}$

ΔC_D	drag due to lift, $C_D - C_{DCL=0}$
q	dynamic pressure, $\frac{1}{2}\rho V^2$, lb/sq ft
S	wing area, sq ft
\bar{c}	mean aerodynamic chord, $\frac{2}{S} \int_0^{b/2} c^2 dy$, ft
c	local wing chord, ft
b	span, ft
ρ	air density, slugs/cu ft
V	free-stream velocity, ft/sec
M	Mach number
R	Reynolds number of wing based on \bar{c}
α	angle of attack, deg
$\Delta\alpha$	local angle-of-attack change due to distortion of wing, deg
K	correction factor for $C_{L\alpha}$ due to wing distortion
$C_{L\alpha}$	lift-curve slope, $\frac{\partial C_L}{\partial \alpha}$
$\Delta \left(\frac{\partial c_m}{\partial C_L} \right)$	incremental change in aerodynamic-center location due to wing distortion
y	spanwise station, ft
$\Lambda_{c/4}$	sweep angle of quarter-chord line
A	aspect ratio, b^2/S

Subscripts:

F	fuselage alone
WF	wing fuselage
BP	base pressure

MODELS AND APPARATUS

The wing-fuselage combinations tested are shown in figure 1. All wings had NACA 65A006 airfoil sections parallel to the fuselage center line and were attached in the midwing position to the aluminum fuselage used with the wings of reference 7. All wings were constructed of aluminum alloy except the 45° sweptback wing (aspect-ratio-4 wing, ref. 7) which was of composite construction, consisting of a steel core with a bismuth-tin covering.

The wings of this investigation represent only a part of the family of wings being studied in a more extensive program; therefore, the wing designation system used in reference 7 is followed herein. For example, the wing designated by 45-4-0.6-006 has the quarter-chord line swept back 45° , an aspect ratio of 4, and a taper ratio of 0.6. The number 006 refers to the section designation - in this case, the design lift coefficient is zero and the thickness is 6 percent of the chord.

The models were tested on the sting-type support system shown in figure 2. With this support system the model can be remotely operated through a 28° angle range. The internally mounted strain-gage balance used to measure wing-fuselage forces and moments is shown installed in a wing-fuselage combination in figure 3.

TESTS AND CORRECTIONS

The tests were conducted in the Langley high-speed 7- by 10-foot tunnel and consisted of measurements of lift, drag, and pitching moment through a Mach number range from approximately 0.4 to 0.95 and through an angle-of-attack range from -2° to 26° . The size of the models used caused the tunnel to choke at corrected Mach numbers of 0.94 to 0.96, depending on the wing being tested.

Blocking corrections, which were applied to the Mach numbers and dynamic pressure were determined by the method of reference 8.

CONFIDENTIAL

Jet-boundary corrections, applied to the lift and drag, were calculated by the method of reference 9. The jet-boundary correction to pitching moment was considered negligible.

No tare corrections were obtained; however, previous experience (ref. 10, for example) indicates that for a tailless sting-mounted model, similar to the models investigated herein, the tare corrections to lift and pitching moment are negligible. The drag data have been corrected to correspond to a pressure at the base of the fuselage equal to free-stream static pressure. For this correction, the base pressure was determined by measuring the pressure inside the fuselage at a point about 9 inches forward of the base. The following corrections were added to the measured drag coefficients:

M	$C_{D_{BP}}$
0.4	0.0015
.6	.0017
.8	.0030
.9	.0033
.95	.0033

The angle of attack has been corrected for deflection of the sting-support system under load.

The test wings were known to deflect under load. Accordingly, in an effort to correct the measured data to the rigid case, correction factors for the effects of the aeroelastic distortion were determined. In an attempt to approximate the distortion of the wing, an elliptical load distribution was simulated by applying loads at four spanwise points along the quarter-chord line of each wing. The resulting spanwise variation in angle of attack $\Delta\alpha$ was measured (fig. 4) and strip theory was used to calculate the effect of this angle-of-attack variation on the lift and lift distribution from which the correction factors of figure 5 were determined. A discussion of the derivation of these corrections is given in reference 7. Results from independent calculations using beam theory and including the effects of aeroelastic distortion on the span load distribution are in good agreement with the results obtained by this analysis.

The mean Reynolds number variation with Mach number for the wings tested is presented in figure 6.

RESULTS AND DISCUSSION

The results of the investigation are presented in the following figures:

	Figures
Basic data.	7 to 9
Summary plots:	
Effects of Mach number.	10 to 14
Effects of sweep.	15 to 16
Minimum drag.	17 to 18
Drag due to lift.	19 to 20
Lift-drag ratios.	21

The basic data for the 45° sweptback wing and the fuselage alone were previously presented in reference 7.

Lift Characteristics

Corrections for the effect of aeroelastic distortion have not been applied to the basic data presented in figures 7 to 9. The lift-curve slopes, measured near zero lift, are presented with and without corrections applied in figures 10 to 14. The correction increases rapidly with increasing sweep, particularly at the higher sweep angles.

The corrected experimental wing-fuselage lift-curve slopes are compared with theory in figures 10 to 13. The theoretical results presented here were obtained by evaluating at zero Mach number the increment of $C_{L\alpha}$ due to the fuselage and wing-fuselage interference from the wing-fuselage theory of reference 11 and applying this increment to the wing-alone theory of reference 12 throughout the Mach number range as follows:

$$(C_{L\alpha_{WF}})_M = (C_{L\alpha_W})_M + \left[(C_{L\alpha_{WF}})_{M=0} - (C_{L\alpha_W})_{M=0} \right]$$

The predictions obtained by this method are in good agreement with the experimental data except at the highest Mach numbers where the predicted effects of compressibility are somewhat too small. The theoretically predicted variation of $C_{L\alpha}$ with Mach number is obtained entirely

from reference 12, since the fuselage increment is constant. The results therefore are in accord with previous data which also has indicated that reference 12 predicts somewhat smaller effects of Mach number than are obtained by experiment. (See for example refs. 3, 7, and 13.)

As has been noted in previous investigations, increases in sweep angle increase the force-break Mach number and decrease the severity of the break.

The variation of lift-curve with sweep at several Mach numbers is compared in figure 15 with theory and the wing-alone data of reference 4. The modified wing-fuselage theory and the wing-alone theory of reference 12, when compared at a Mach number of 0.4, are not greatly different from each other and each is in good agreement with the experimental results. Considering this good agreement and the involved calculation required by the modified wing-fuselage theory, the wing-alone theory of reference 12 could probably be used satisfactorily for a general estimation of wing-fuselage lift-curve slopes for models similar to the one used in the present investigation.

Pitching-Moment Characteristics

The basic data (figs. 7 to 9) have not been corrected for the effects of aeroelastic distortion. The summary plots (figs. 10 to 14) present the slopes of the pitching-moment curve, measured near zero lift, with and without corrections for distortion. The corrections increase rapidly with an increase in the sweep angle.

Below the force-break Mach number the aerodynamic-center location, as expressed by the slope $\partial C_m / \partial C_L$, remains relatively constant (fig. 14); however, above this point a rapid rearward movement occurs, as expected. The reversal of this rearward movement for the unswept wing at a Mach number of 0.91 is probably due to shock-stall separation.

The corrected aerodynamic-center locations $\partial C_m / \partial C_L$ are compared with theory in figures 10 to 13 and 16. The theory of reference 12 was modified by the same procedure indicated previously for lift-curve slope. The resulting wing-fuselage theoretical values are in good agreement with the experimental data at Mach numbers below the force break except for the 60° swept wing. It should be noted that at this sweep angle the wing-alone theory of reference 12, which the modified wing-fuselage theory uses as a basis, also predicts a more rearward location (fig. 16) than shown by the wing-alone data of reference 4.

A comparison of the experimental data of this paper with the data of reference 2 shows some noticeable differences. Some of these differences are associated with the lift-coefficient range over which the slopes were measured and the number of data points available for establishing the slopes in reference 2. Similar differences are noted and discussed in reference 6.

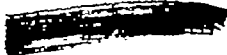
At moderate lift coefficients the pitching-moment curves of the wings of 45° and 60° sweepback (fig. 8 of ref. 7 and fig. 9 of this paper) exhibit destabilizing breaks, with the break for the 60° swept wing being more severe and occurring at a lower lift coefficient than that of the wing of 45° sweep angle. The unswept wing exhibits a stable break, whereas the 32.6° swept wing exhibits a slight erratic variation followed by a stable break at the highest lift coefficients. These effects are in agreement with the correlation presented in reference 14.

Drag Characteristics

Drag at zero lift.— The beneficial effect of increases in sweep angle in increasing the drag-rise Mach number for the wing-fuselage combination can be seen from figure 14. The data for the fuselage alone are presented in reference 7; therefore, only the minimum drag is presented here (fig. 17.) The wing plus wing-fuselage interference-drag data of figure 18 were obtained by subtracting the fuselage-alone drag of figure 17 from the wing-fuselage drag of figure 14. The differences shown below the drag-rise Mach number can be attributed partially to different interference effects and partially to the relative accuracy of the results.

Drag due to lift.— In general, the 60° swept wing has the highest drag due to lift and the 32.6° swept wing the lowest (fig. 19.) It will be noted that all wings exhibit considerably higher drag than predicted by the theory (given approximately by $C_L^2/\pi A$) for the condition of the resultant force normal to the local relative wind. This may indicate the possibility of early loss of leading-edge suction due to leading-edge separation, thereby approaching the condition where the resultant force is normal to the wing-chord plane. At this condition the wings with the lower lift-curve slopes (higher sweep angles) would have the highest drag. These effects are discussed more completely in reference 1.

The drag due to lift of the 45° and 60° swept wings was found to be unaffected by Mach number (fig. 20) while the wings with less sweep showed some effect of Mach number.



Lift-Drag Ratios

Mach number has little effect on the maximum lift-drag ratio below the drag-rise Mach number (fig. 14); above this point a rapid reduction in the maximum lift-drag ratio occurs for all wings. This reduction is primarily associated with the increase in minimum drag at these Mach numbers (fig. 14.) The maximum lift-drag ratio decreases with increasing sweep at Mach numbers below the drag rise. This decrease is due largely to the increase in drag due to lift with increasing sweep.

Increases in sweep reduce the lift coefficient at which the maximum lift-drag ratio occurs (fig. 21). The effect of increasing sweep in providing higher lift-drag ratios over a wide range of lift coefficients at the higher Mach numbers is graphically illustrated in figure 21.

CONCLUSIONS

The results of the investigation at high-subsonic speeds of a series of wings of varying sweep and with an aspect ratio of 4, a taper ratio of 0.6, and an NACA 65A006 airfoil section indicate the following conclusions:

1. The increase of lift-curve slopes with Mach number and the decrease with sweep angle as predicted by available theory are in good agreement with the experimental data.
2. The experimental wing-fuselage aerodynamic center showed little variation with Mach number up to the force-break Mach number. At higher Mach numbers all wings exhibited a rapid rearward movement of the aerodynamic center. By a modification of an available theory the aerodynamic-center locations could be predicted very well for sweep angles up to 45° , except at the highest Mach numbers.
3. In general the drag due to lift and the drag-rise Mach number increased with increasing sweep. The wings with the most sweep showed no effect of Mach number on the drag due to lift within the test range.
4. The maximum lift-drag ratio decreased with an increase in sweep at the low Mach numbers; however, at the highest Mach number increases in sweep gave large increases in lift-drag ratio over a

wide range of lift coefficients. All wings exhibited a marked decrease in maximum lift-drag ratio above the drag-rise Mach number.

Langley Aeronautical Laboratory
National Advisory Committee for Aeronautics
Langley Field, Va.

REFERENCES

1. Polhamus, Edward C.: Summary of Results Obtained by Transonic-Bump Method on Effects of Plan Form and Thickness on Lift and Drag Characteristics of Wings at Transonic Speeds. NACA RM L51H30, 1951.
2. Luoma, Arvo A.: Aerodynamic Characteristics of Four Wings of Sweepback Angles 0° , 35° , 45° , and 60° , NACA 65A006 Airfoil Section, Aspect Ratio 4, and Taper Ratio 0.6 in Combination With a Fuselage at High Subsonic Mach Numbers and at a Mach Number of 1.2. NACA RM L51D13, 1951.
3. Sutton, Fred B., and Martin, Andrew: Aerodynamic Characteristics Including Pressure Distributions of a Fuselage and Three Combinations of the Fuselage With Sweptback Wings at High Subsonic Speeds. NACA RM A50J26a, 1951.
4. Cahill, Jones F., and Gottlieb, Stanley M.: Low-Speed Aerodynamic Characteristics of a Series of Swept Wings Having NACA 65A006 Airfoil Sections. NACA RM L50F16, 1950.
5. Letko, William, and Wolhart, Walter D.: Effect of Sweepback on the Low-Speed Static and Rolling Stability Derivatives of Thin Tapered Wings of Aspect Ratio 4. NACA RM L9F14, 1949.
6. Donlan, Charles J., Myers, Boyd C., II, and Mattson, Axel T.: A Comparison of the Aerodynamic Characteristics at Transonic Speeds of Four Wing-Fuselage Configurations as Determined From Different Test Techniques. NACA RM L50H02, 1950.
7. Kuhn, Richard E., and Wiggins, James W.: Wind-Tunnel Investigation of the Aerodynamic Characteristics in Pitch of Wing-Fuselage Combinations at High Subsonic Speeds. Aspect-Ratio Series. NACA RM L52A29, 1952.
8. Hensel, Rudolph W.: Rectangular-Wind-Tunnel Blocking Corrections Using the Velocity-Ratio Method. NACA TN 2372, 1951.
9. Gillis, Clarence L., Polhamus, Edward C., and Gray, Joseph L., Jr.: Charts for Determining Jet-Boundary Corrections for Complete Models in 7- by 10- Foot Closed Rectangular Wind Tunnels. NACA ARR L5G31, 1945.

CONFIDENTIAL

~~CONFIDENTIAL~~

10. Osborne, Robert S.: High-Speed Wind-Tunnel Investigation of the Longitudinal Stability and Control Characteristics of a $\frac{1}{16}$ -Scale Model of the D-558-2 Research Airplane at High Subsonic Mach Numbers and at a Mach Number of 1.2. NACA RM L9C04, 1949.
11. McLaughlin, Milton D.: Method of Estimating the Stick-Fixed Longitudinal Stability of Wing-Fuselage Configurations Having Unswept and Swept Wings. NACA RM L51J23, 1952.
12. DeYoung, John: Theoretical Additional Span Loading Characteristics of Wings With Arbitrary Sweep, Aspect Ratio, and Taper Ratio. NACA TN 1491, 1947.
13. Murray, Harry E.: Comparison with Experiment of Several Methods of Predicting the Lift of Wings in Subsonic Compressible Flow. NACA TN 1739, 1948.
14. Shortal, Joseph A., and Maggin, Bernard: Effect of Sweepback and Aspect Ratio on Longitudinal Stability Characteristics of Wings at Low Speeds. NACA TN 1093, 1946.

~~CONFIDENTIAL~~

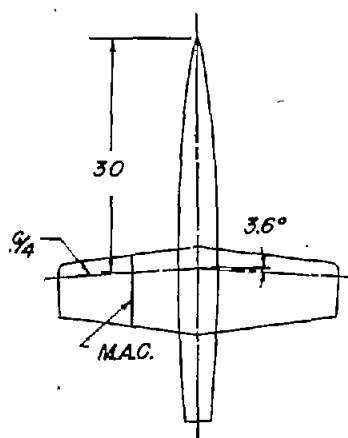
Fuselage:

Length 49.2 in.
Max. diam. 5 in.
Position of max. diam. 30 in.

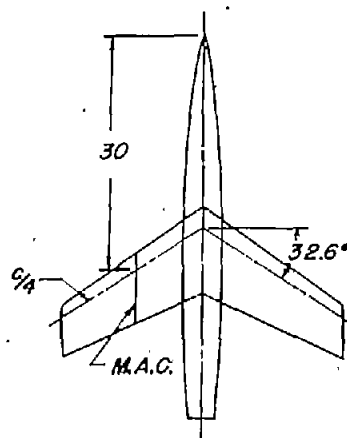
Wing:

Area 2.25 sqft
Span 3.0 ft
Chord
Tip 6.75 in.
Root 11.25 in.
Mean aerodynamic chord .765 ft
Aspect ratio 4
Taper ratio 6
Incidence 0
Dihedral 0
Airfoil section
parallel to fuselage & NACA 65A006

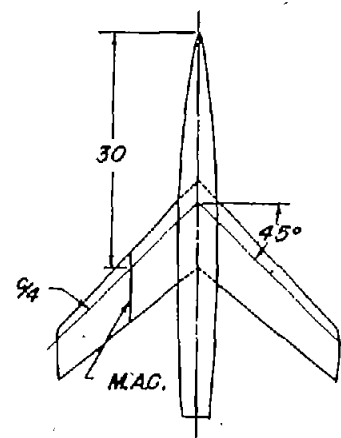
0 10 20
Scale, inches



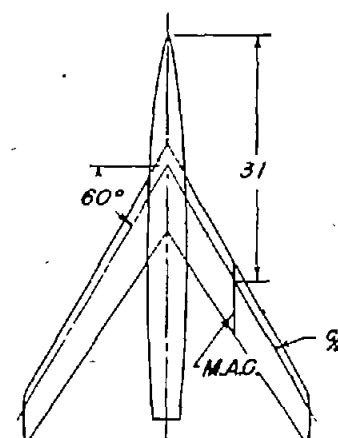
3.6-4-0.6-006



32.6-4-0.6-006



45-4-0.6-006



60-4-0.6-006

Basic data presented in Ref. 6.



Figure 1.- Drawing of the four wing-fuselage configurations.

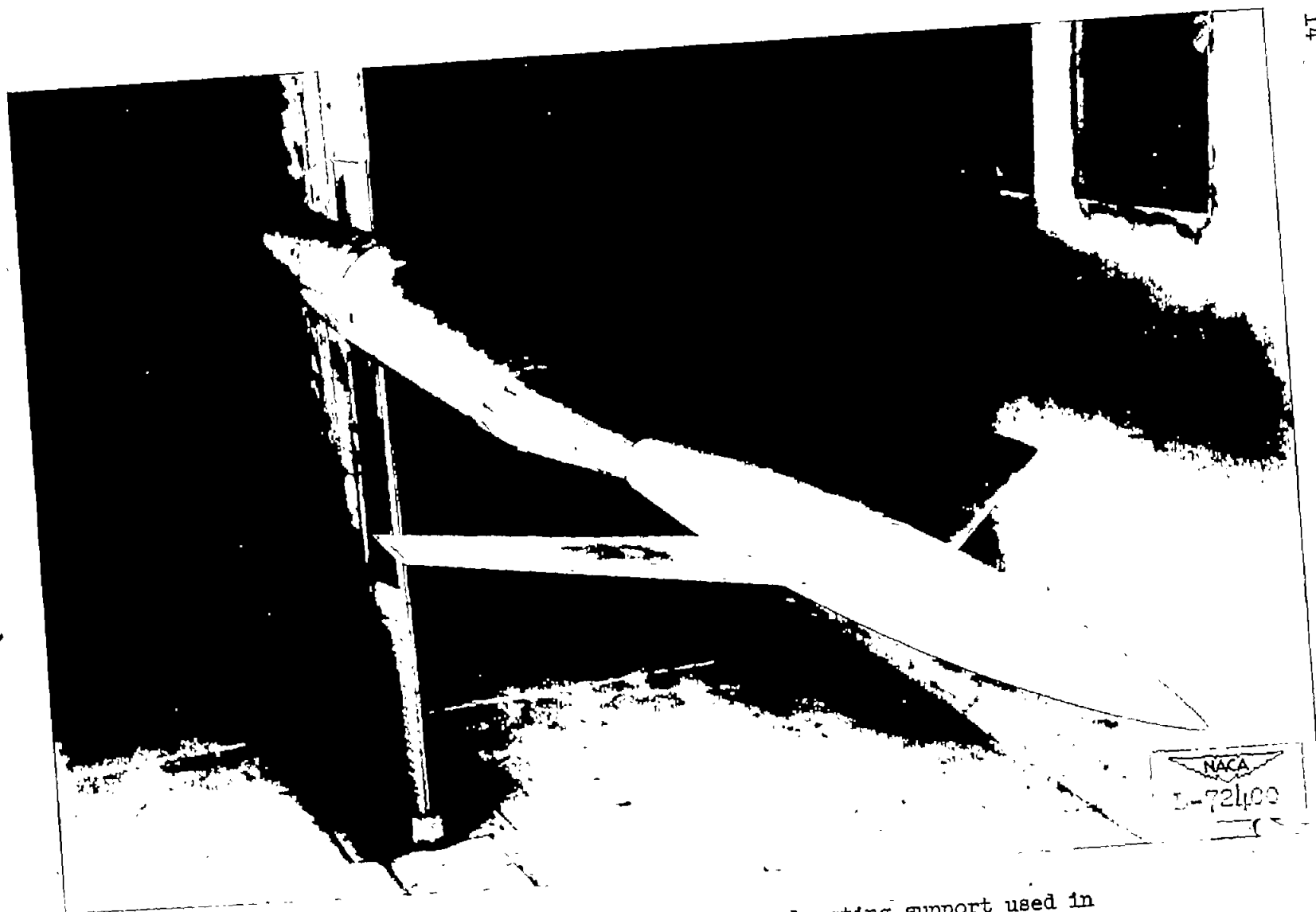


Figure 2.- Model installed on the variable-angle sting support used in the Langley high-speed 7- by 10-foot tunnel.

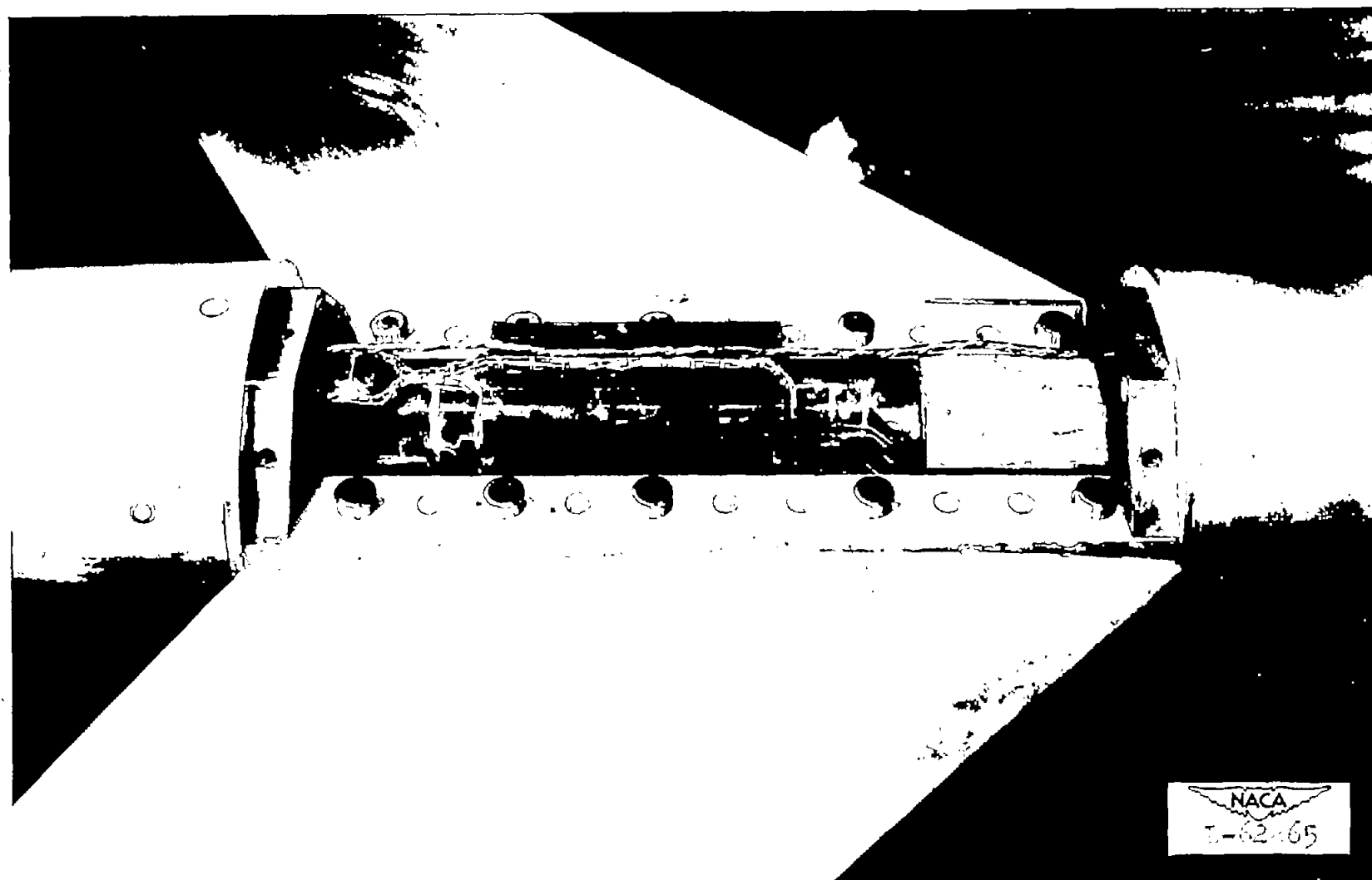


Figure 3.- View of model showing strain-gage balance and some details of model construction.

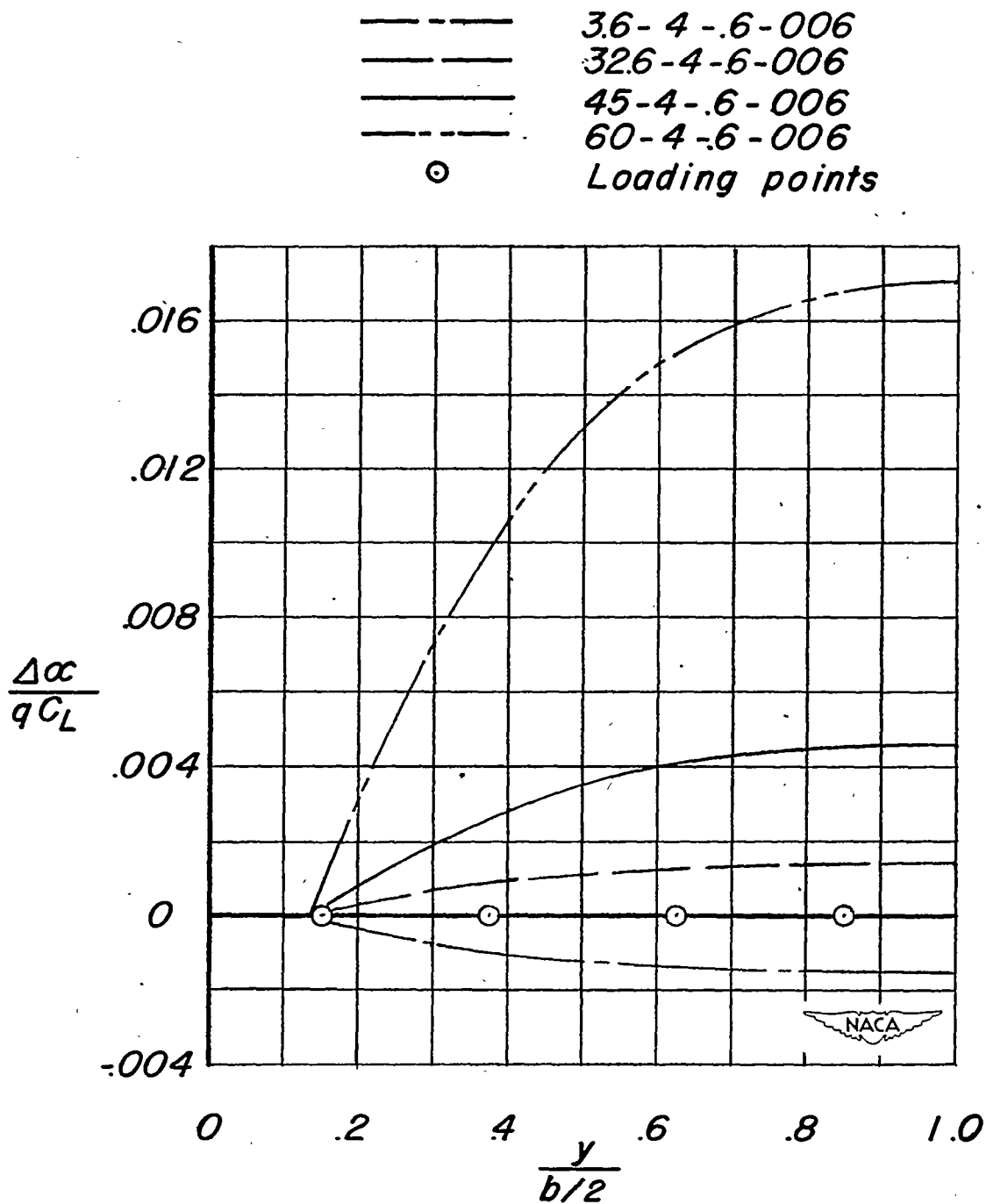


Figure 4.- Spanwise variation of angle of attack due to aeroelastic distortion.

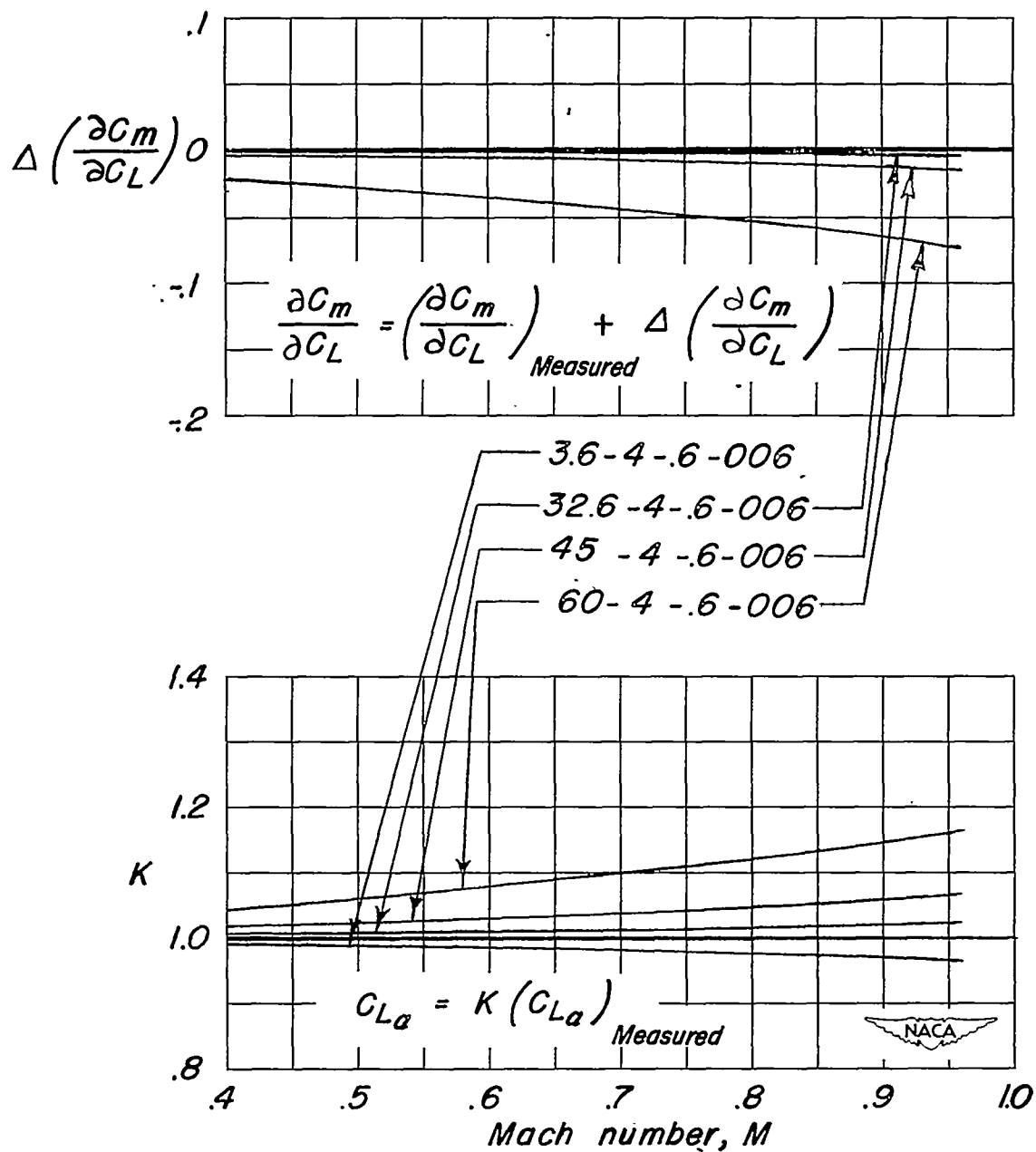


Figure 5.- Correction factors used to correct the summary data for the effects of aeroelastic distortion.

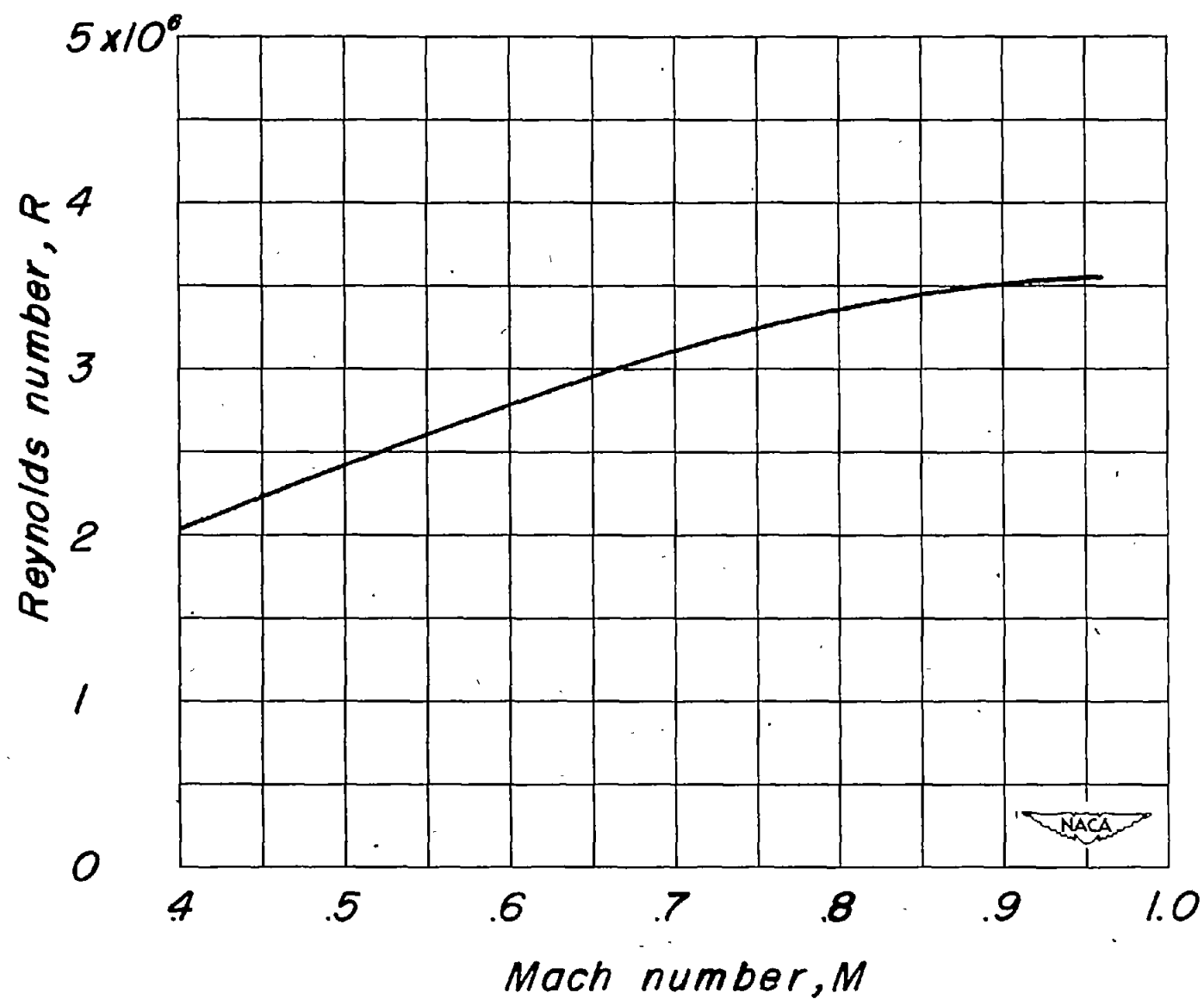
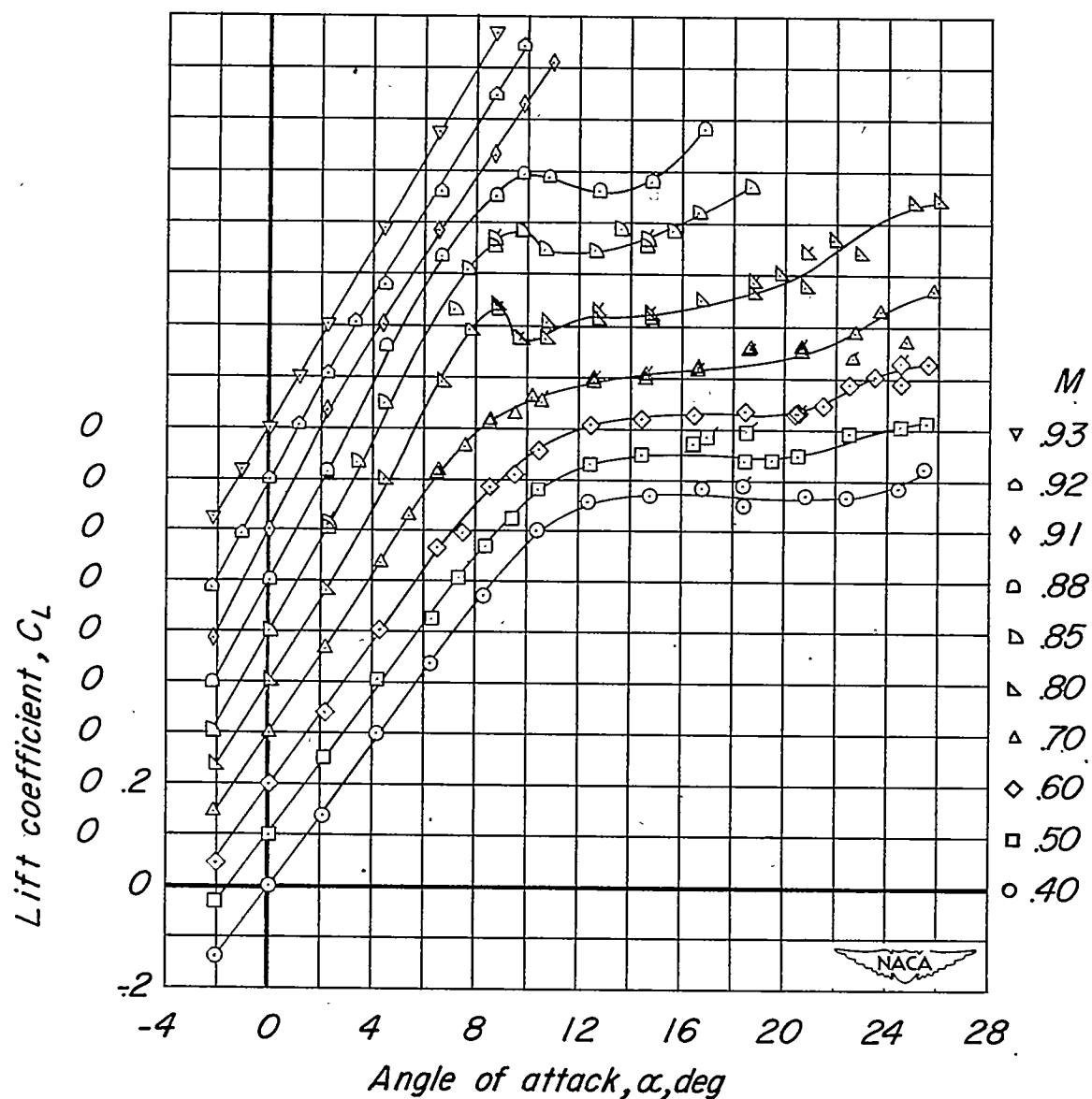
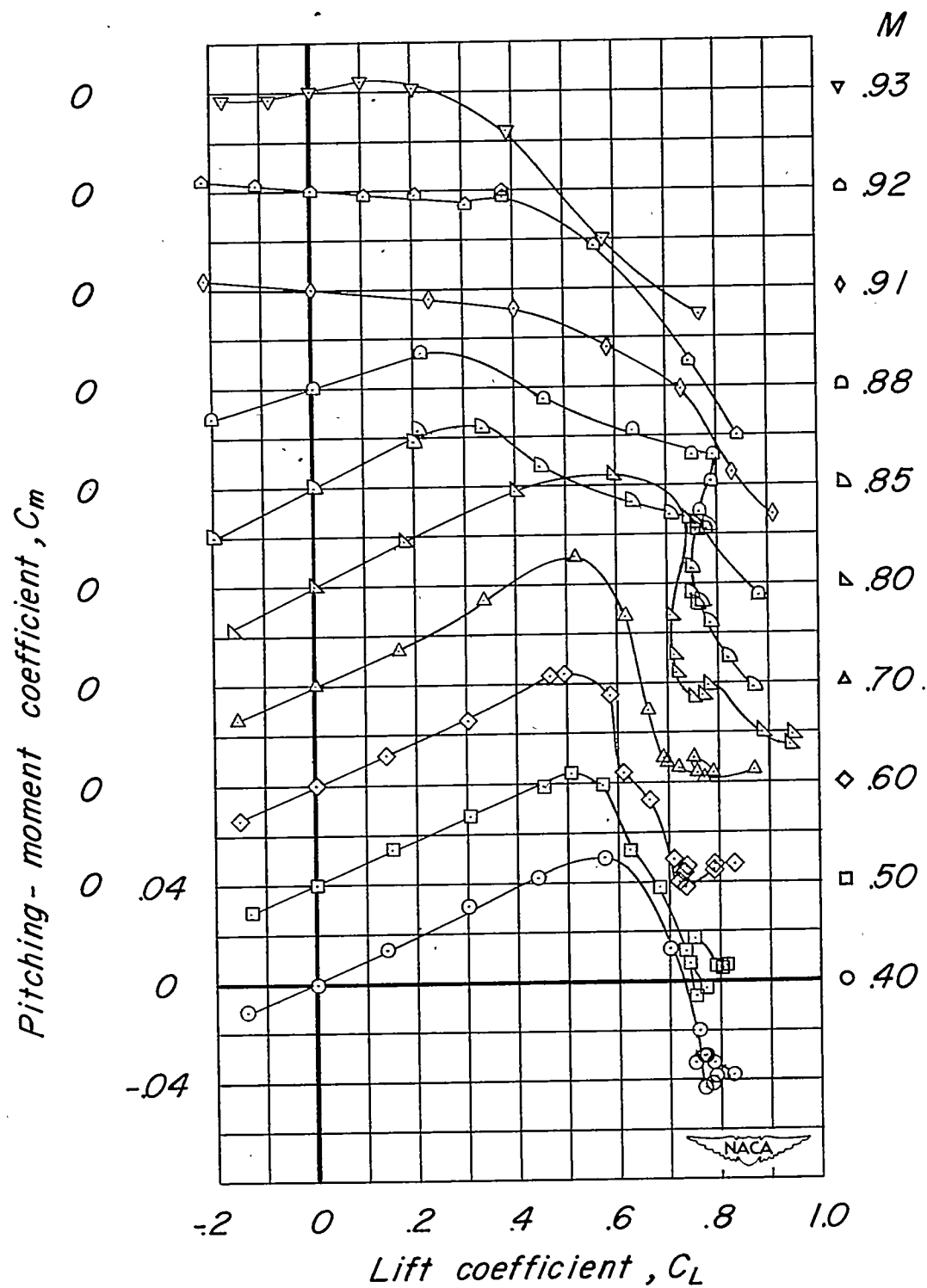


Figure 6.- Variation of mean Reynolds number with Mach number based on the mean aerodynamic chord of 0.765 foot.



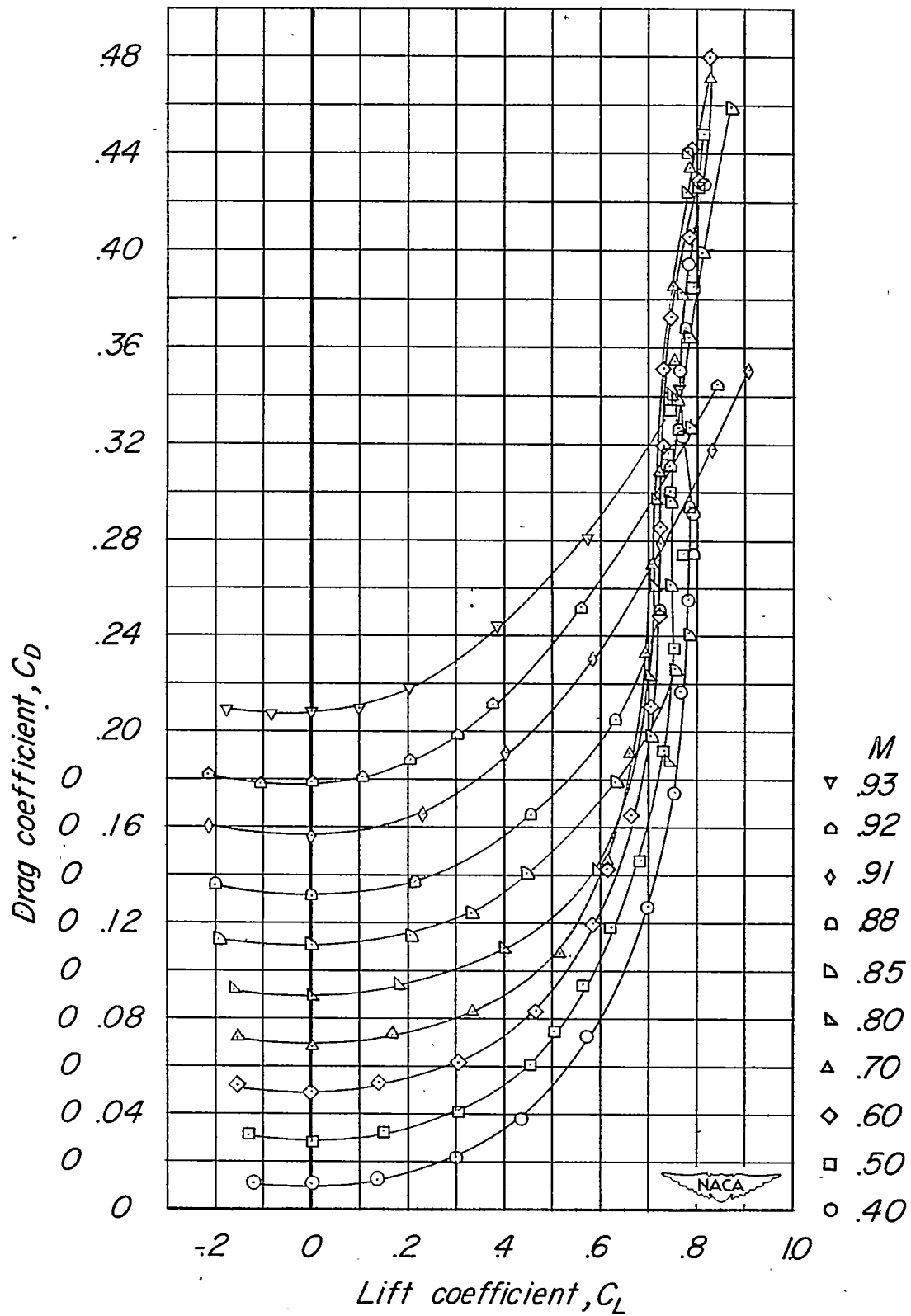
(a) Lift. (3.6-4-0.6-006)

Figure 7.- Aerodynamic characteristics of the 3.6° sweptback wing-fuselage configuration. Not corrected for aeroelastic distortion.



(b) Pitching moment. (3.6-4-0.6-006)

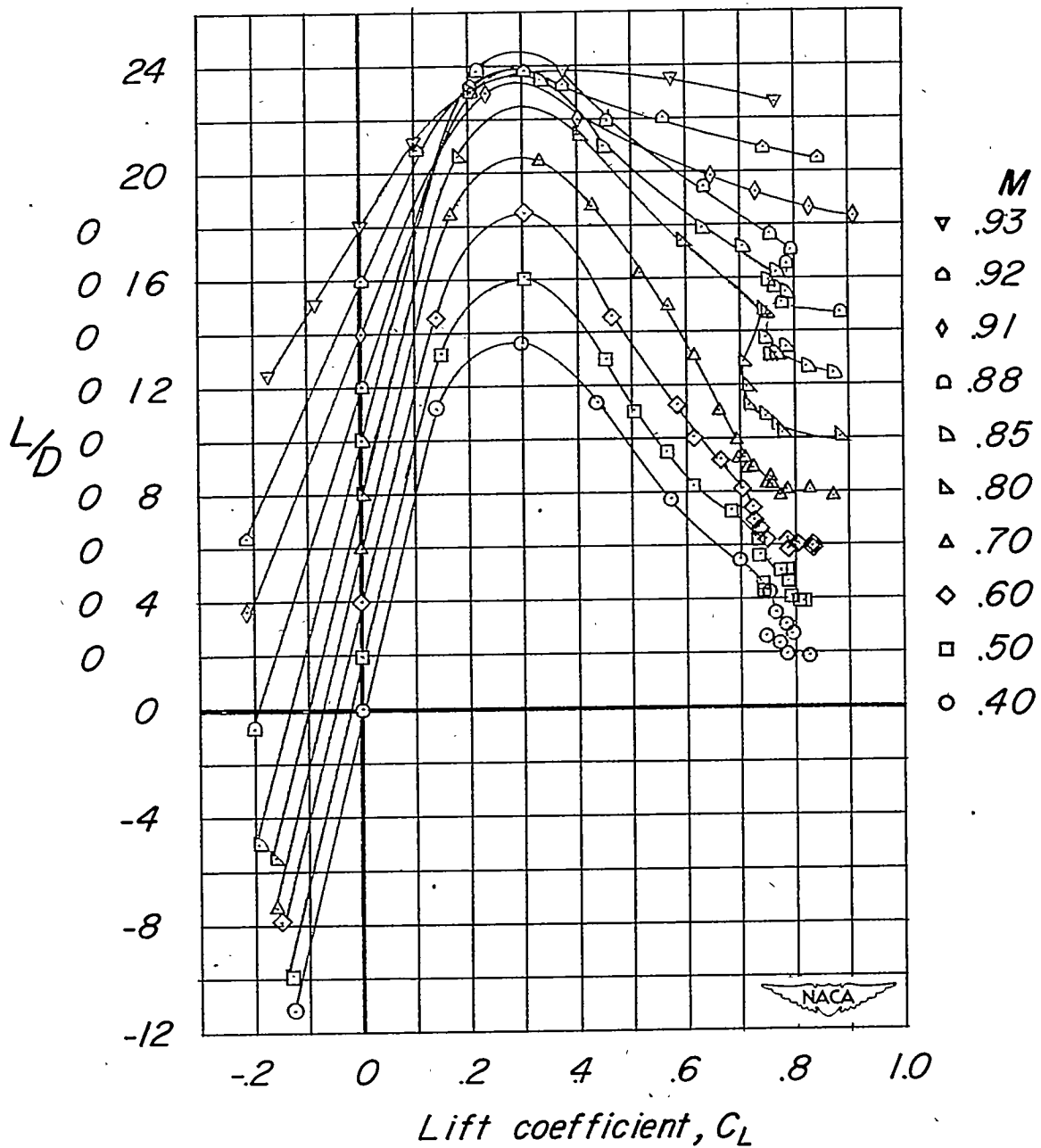
Figure 7.- Continued.



(c) Drag. (3.6-4-0.6-006)

Figure 7.- Continued.

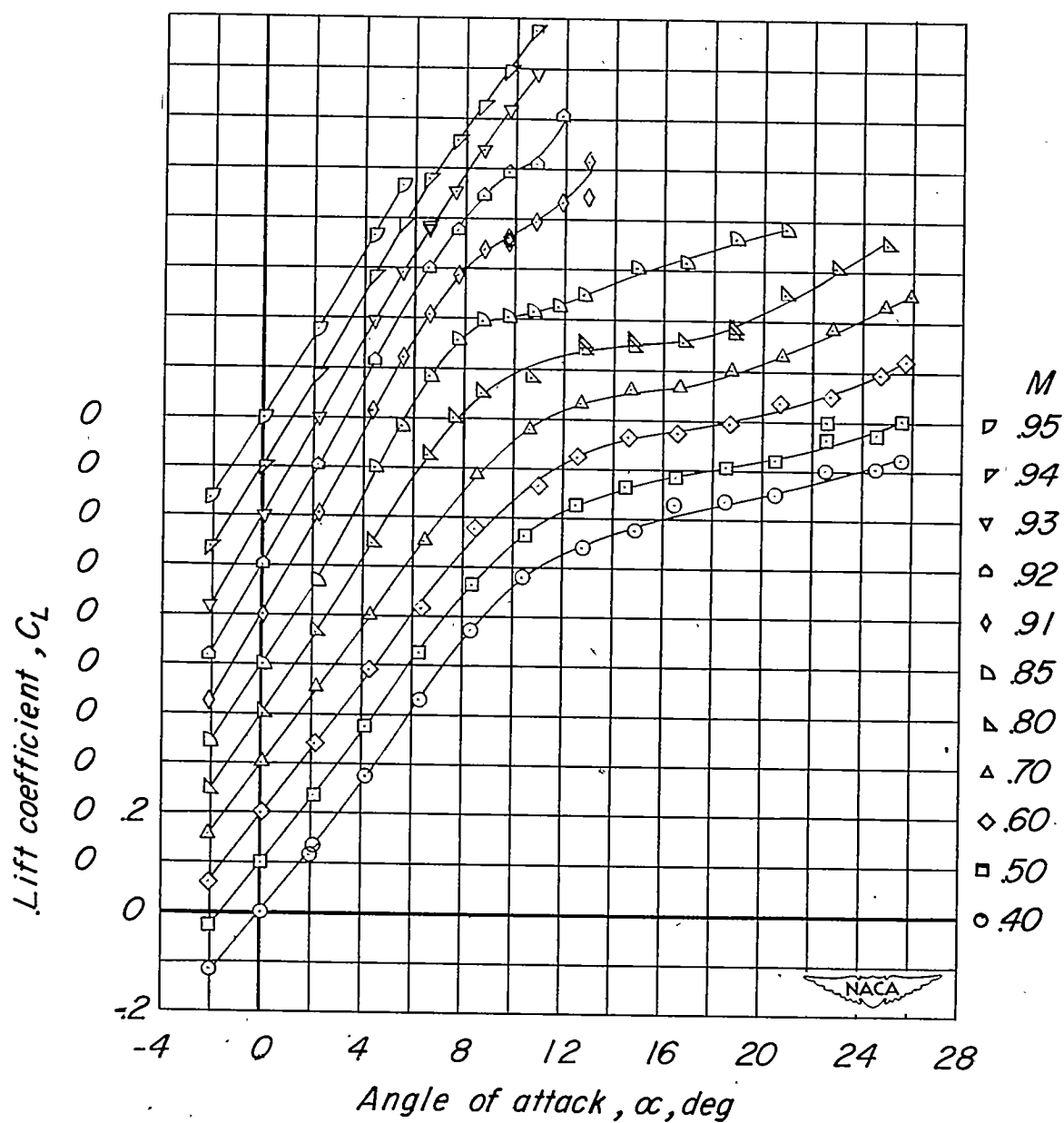
CONFIDENTIAL



(d) Lift-drag ratios. (3.6-4-0.6-006)

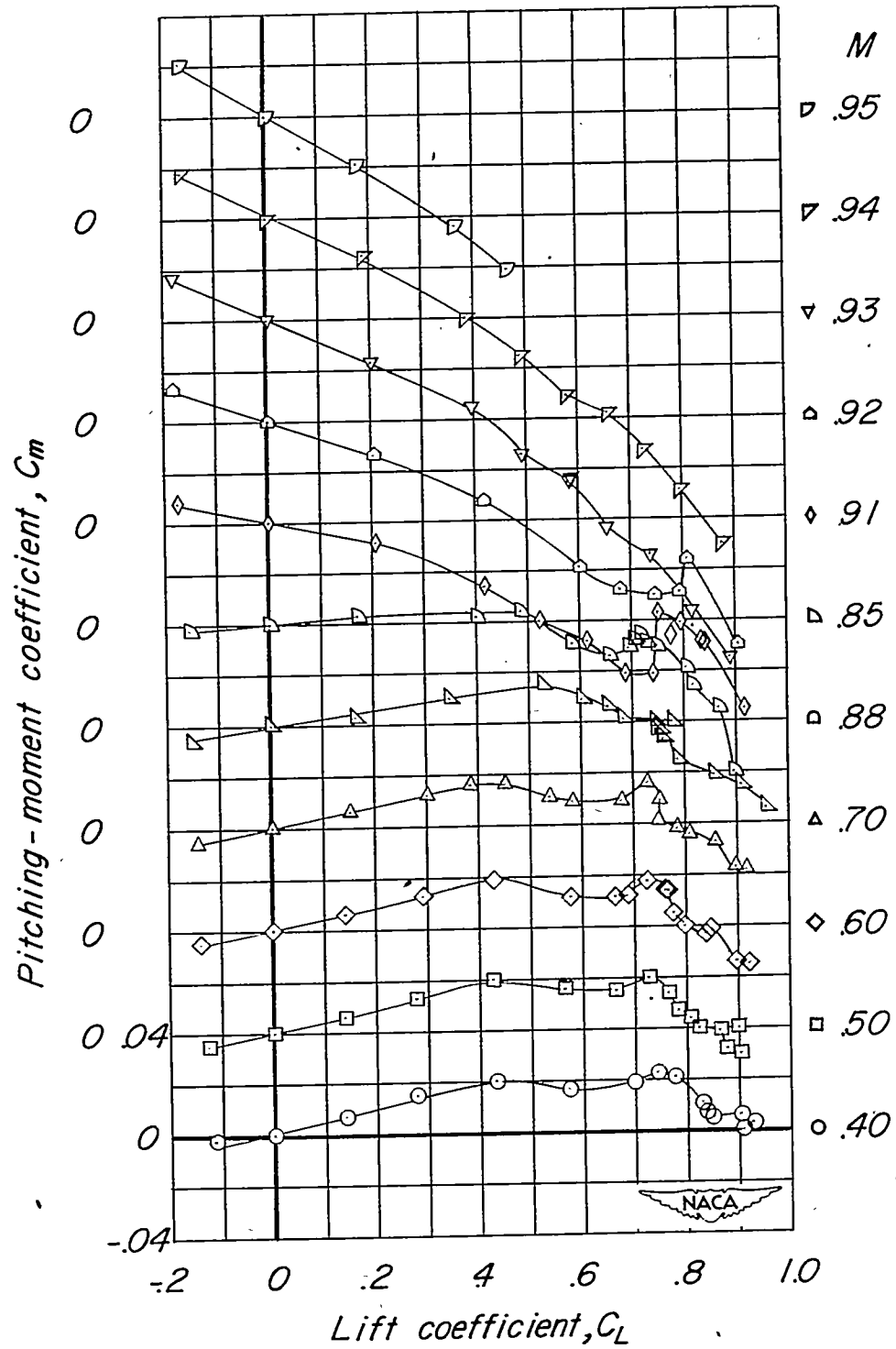
Figure 7.- Concluded.

CONFIDENTIAL



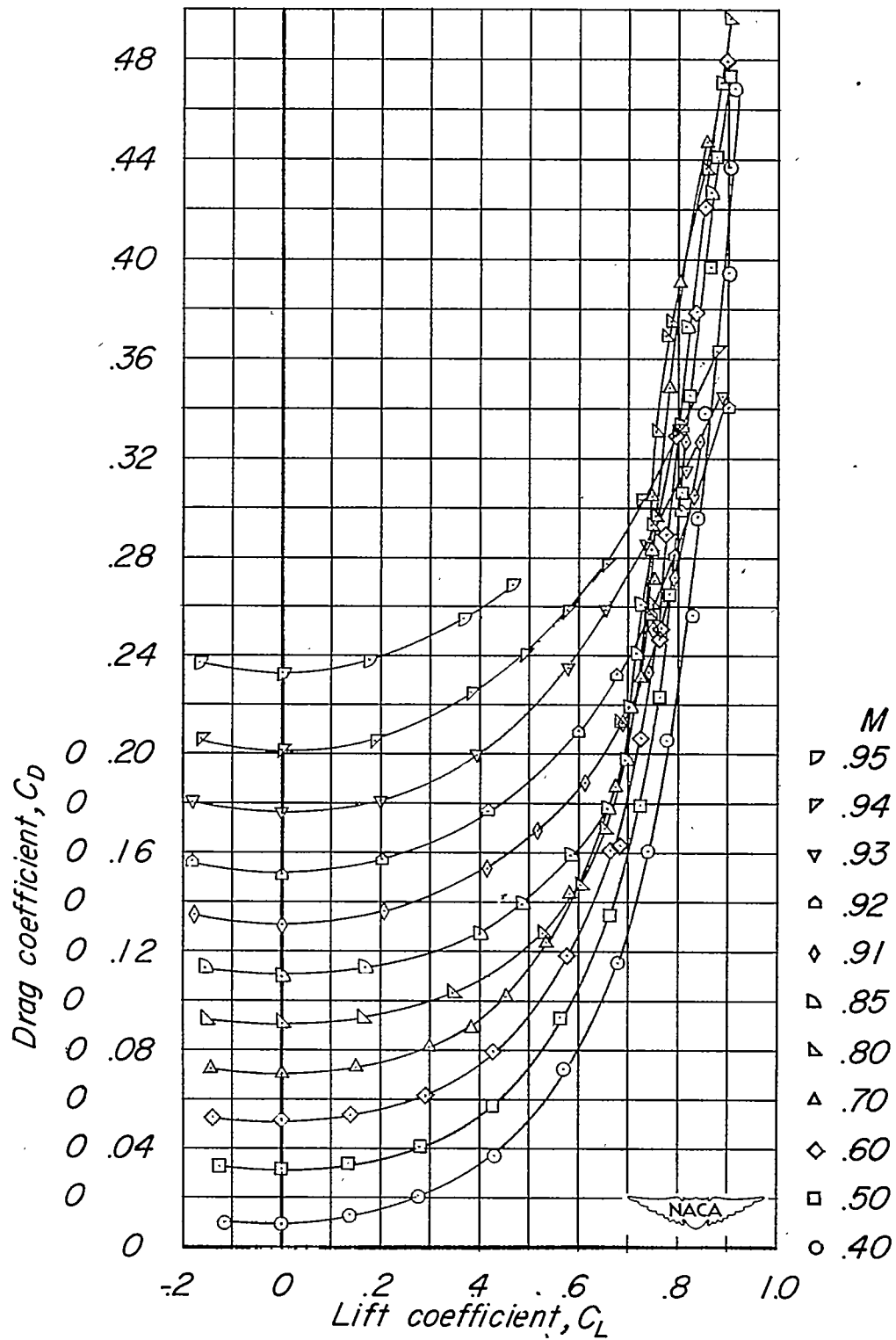
(a) Lift. (32.6-4-0.6-006)

Figure 8.- Aerodynamic characteristics of the 32.6° sweptback wing-fuselage configuration. Not corrected for aeroelastic distortion.



(b) Pitching moment. (32.6-4-0.6-006)

Figure 8.- Continued.

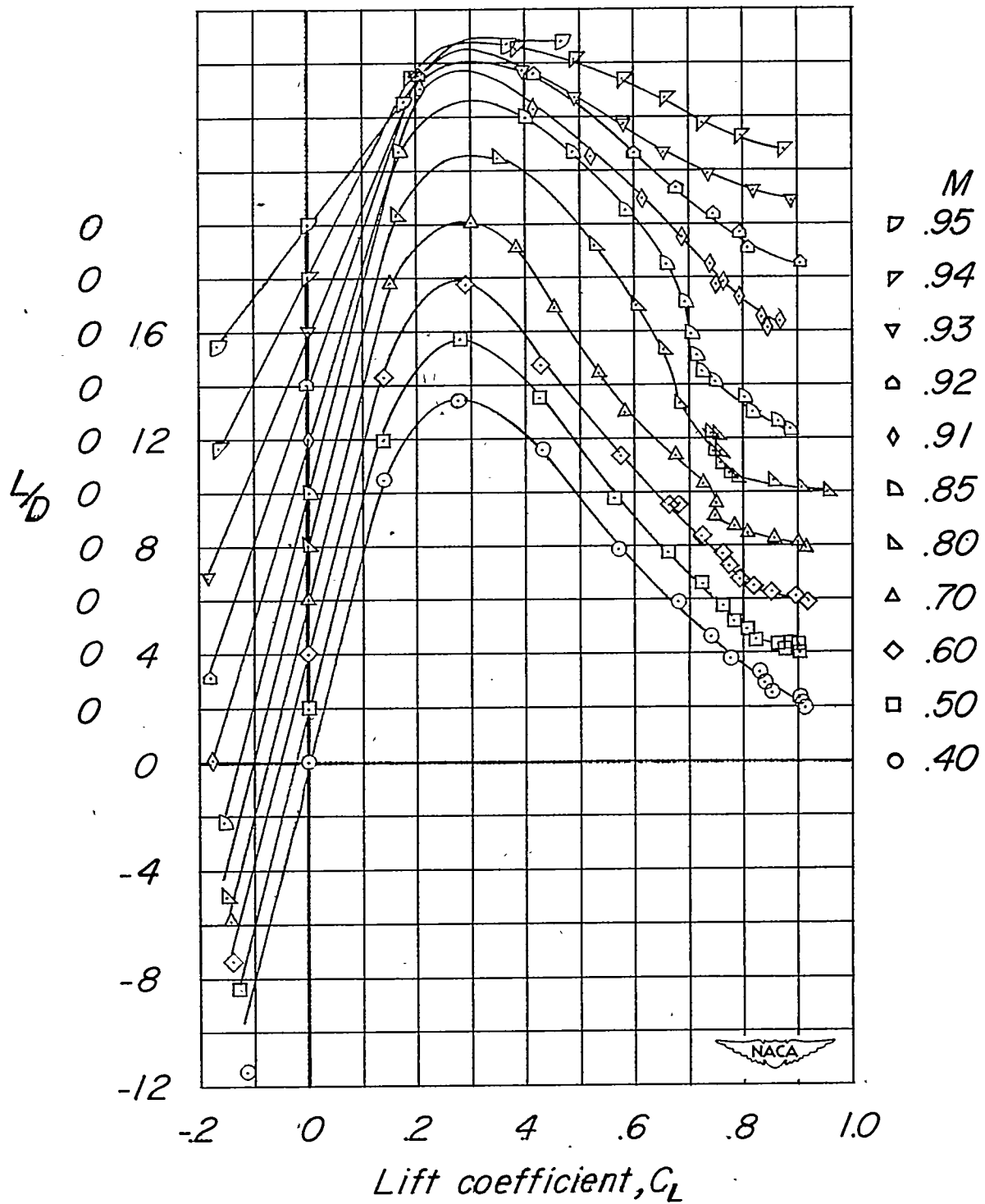
~~CONFIDENTIAL~~

(c) Drag. (32.6-4-0.6-006)

Figure 8.- Continued.

~~CONFIDENTIAL~~

CONFIDENTIAL

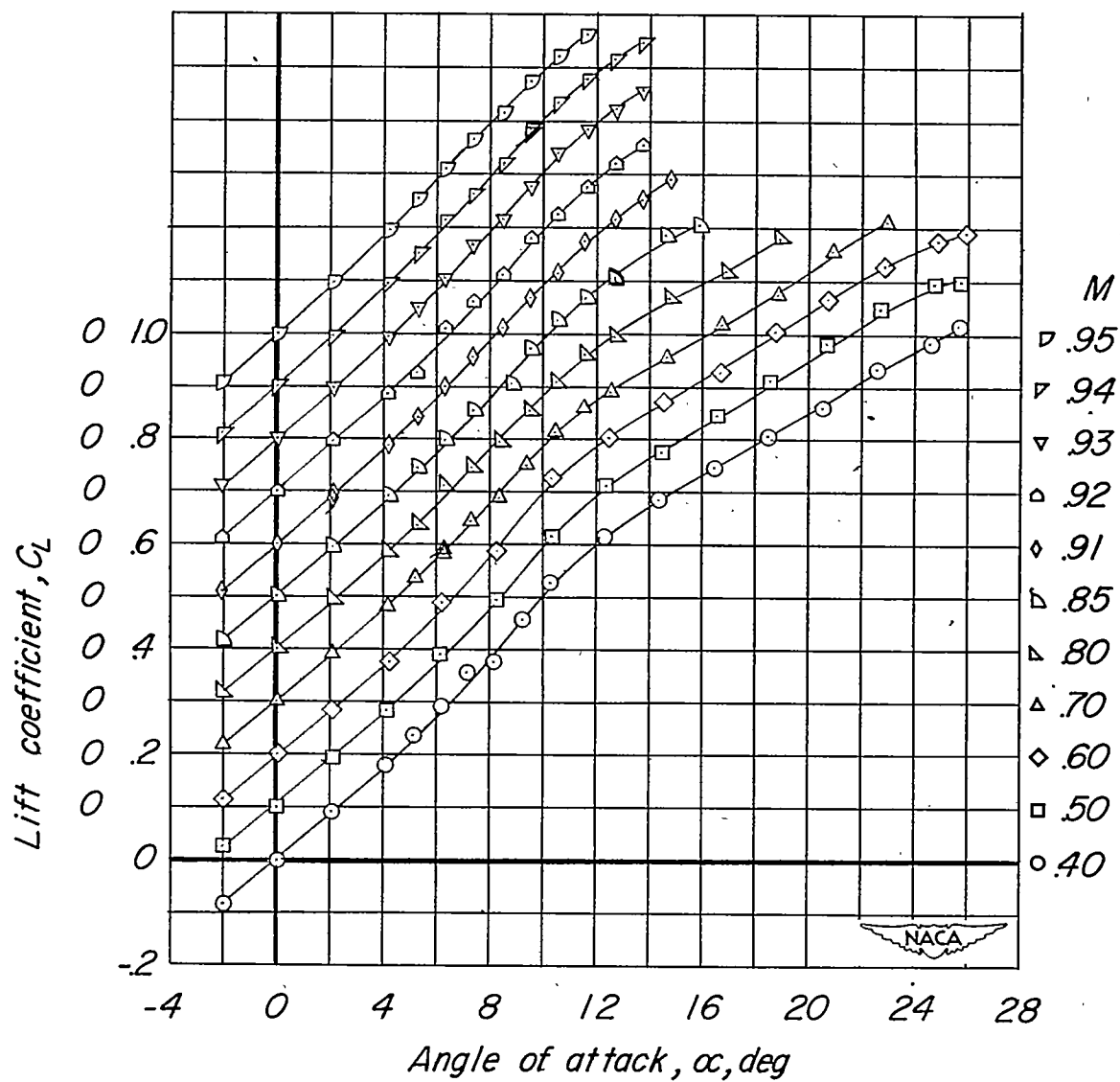


(d) Lift-drag ratios. (32.6-4-0.6-006)

Figure 8.- Concluded.

CONFIDENTIAL

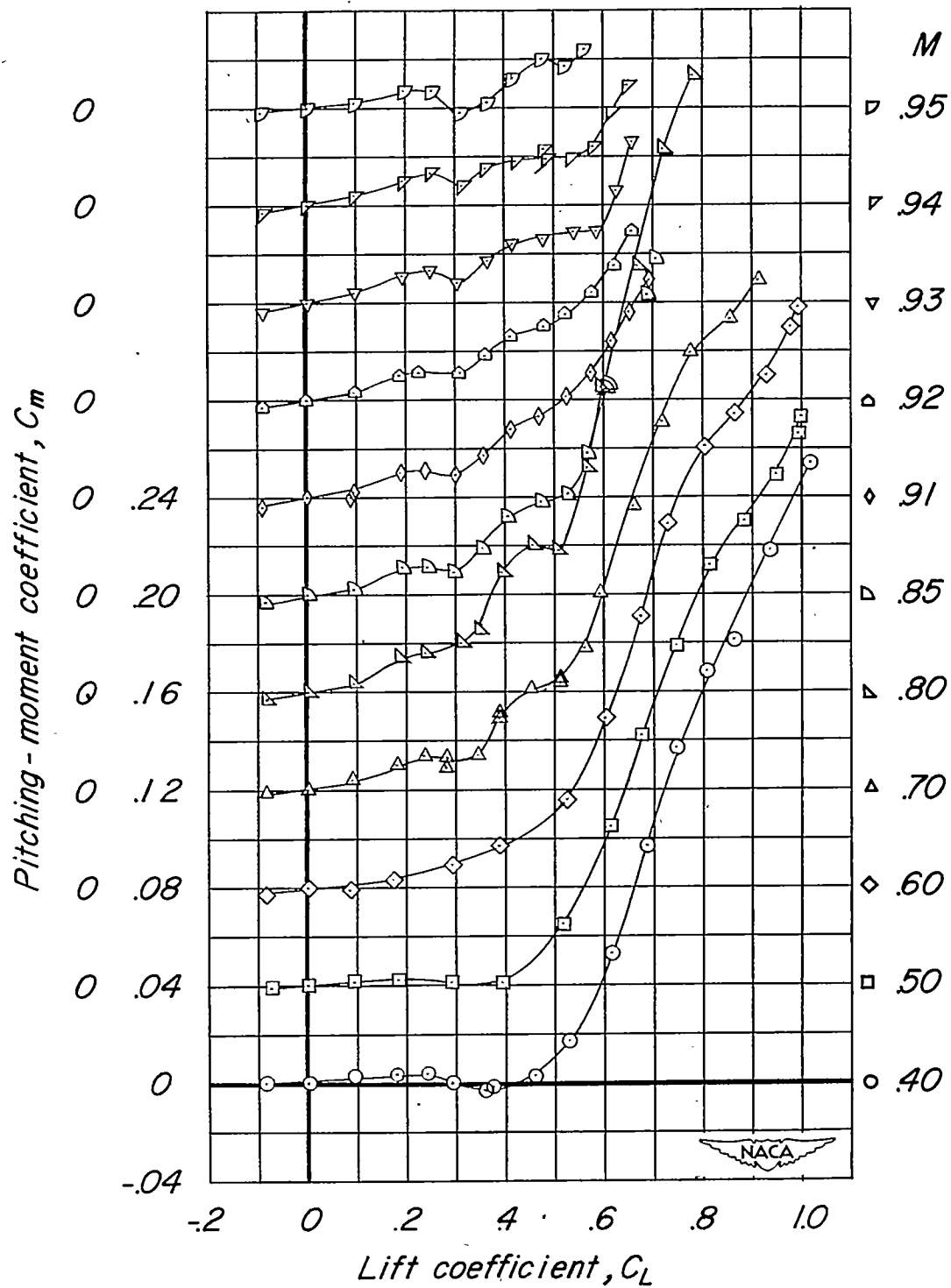
CONFIDENTIAL



(a) Lift. (60-4-0.6-006)

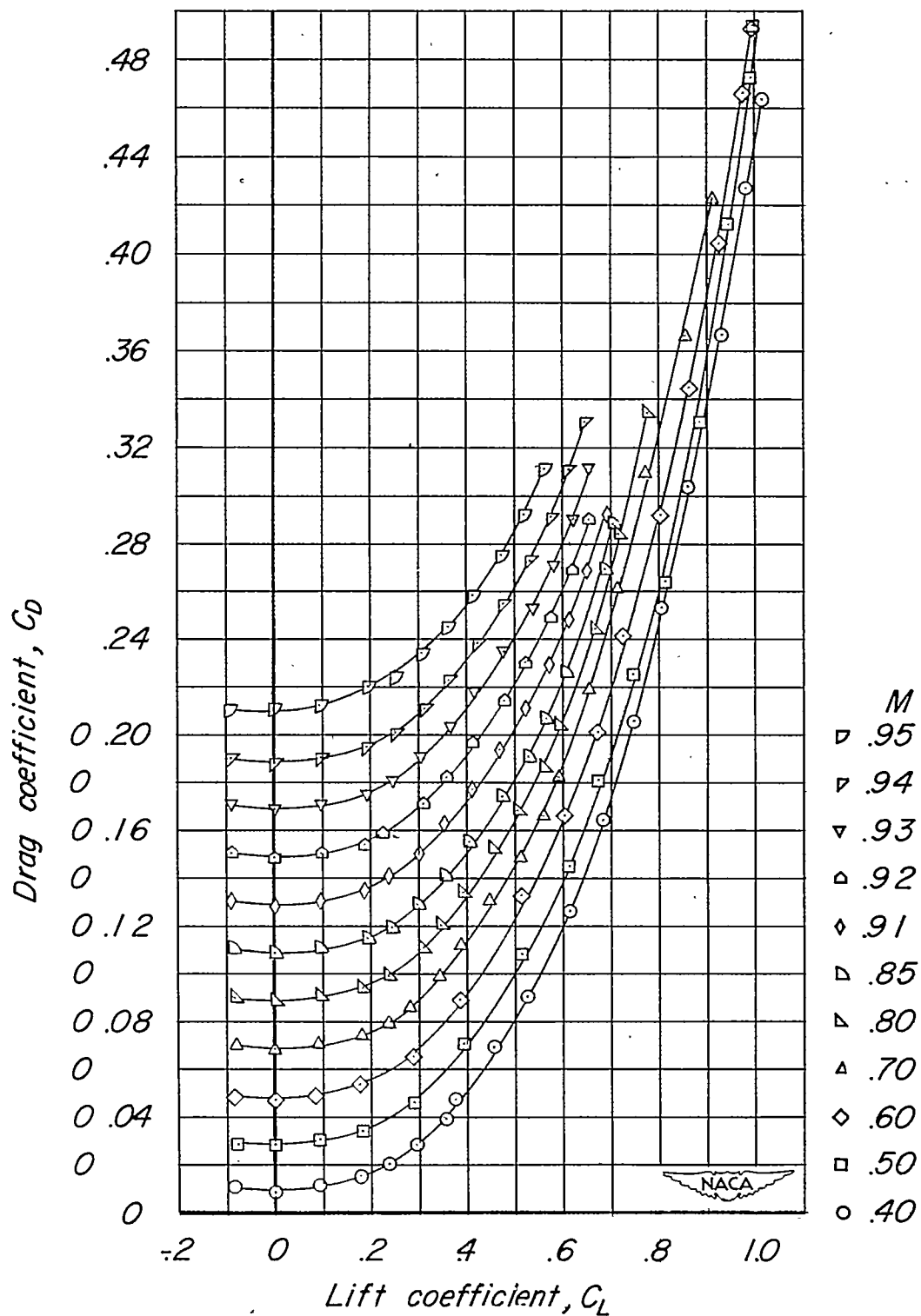
Figure 9.- Aerodynamic characteristics of the 60° sweptback wing-fuselage configuration. Not corrected for aeroelastic distortion.

CONFIDENTIAL



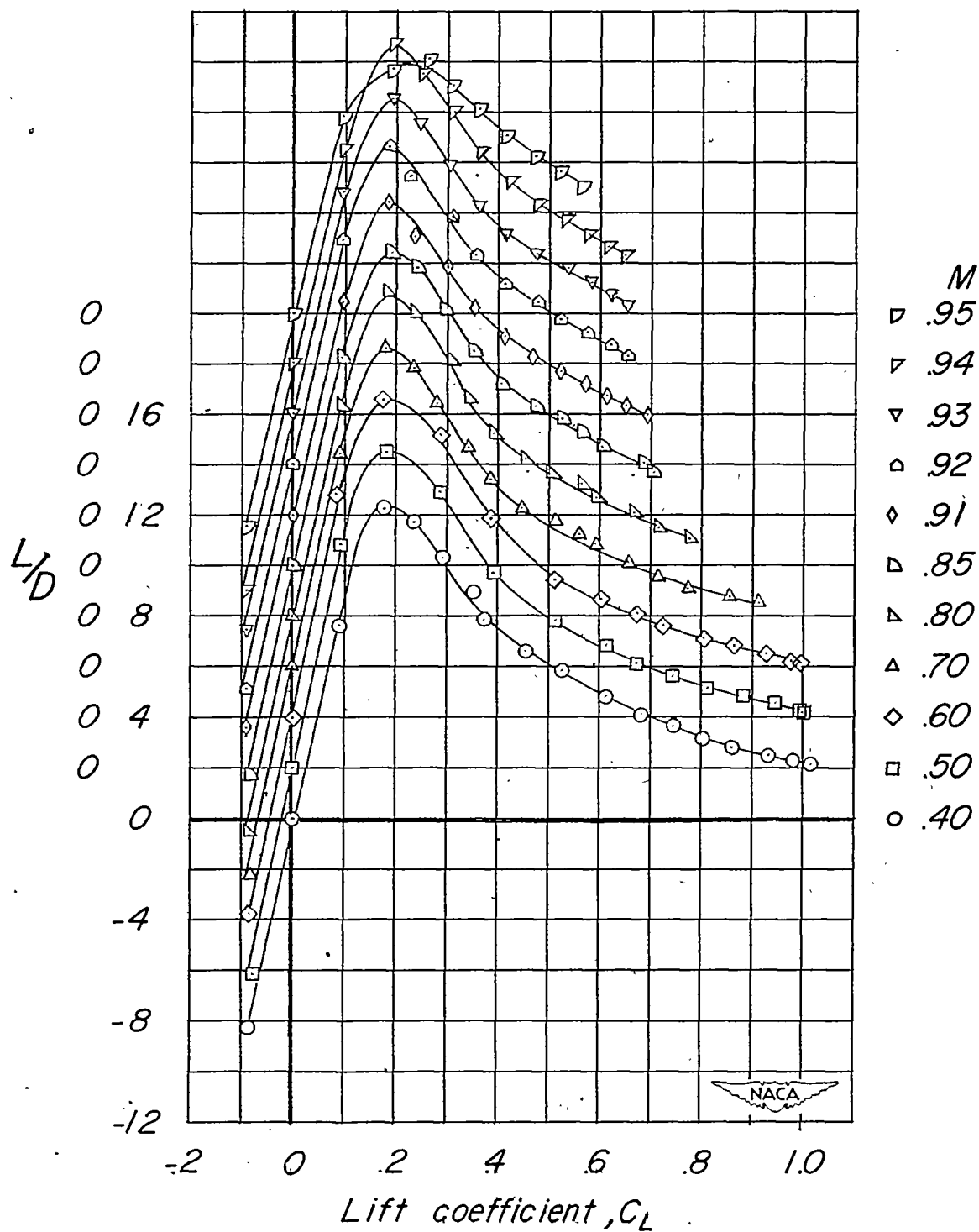
(b) Pitching moment. (60-4-0.6-006)

Figure 9.- Continued.



(c) Drag. (60-4-0.6-006)

Figure 9.- Continued.



(d) Lift-drag ratios. (60-4-0.6-006)

Figure 9.- Concluded.

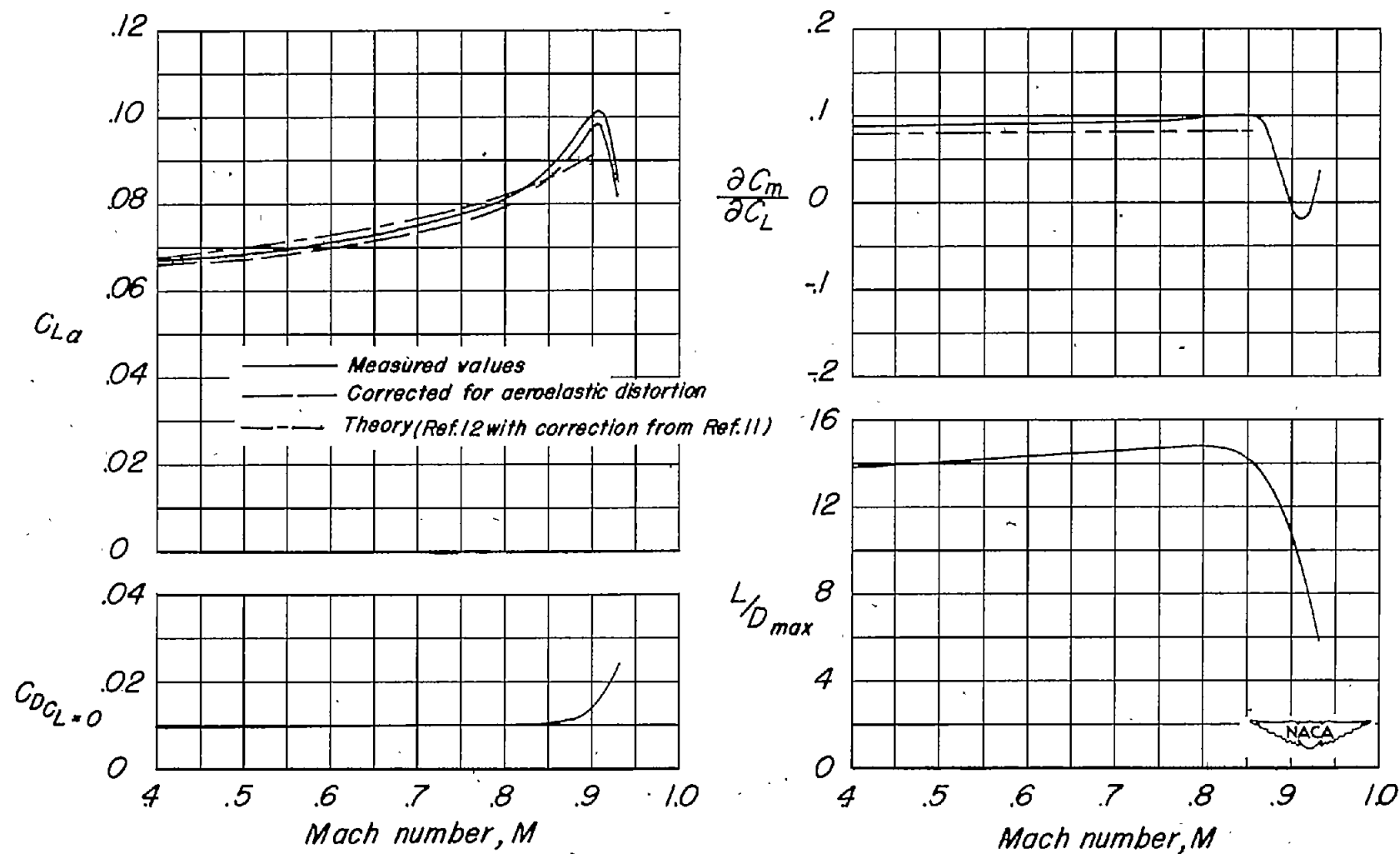


Figure 10.- Summary of the effect of Mach number on the aerodynamic characteristics of the 3.6-4-0.6-006 wing-fuselage combination.

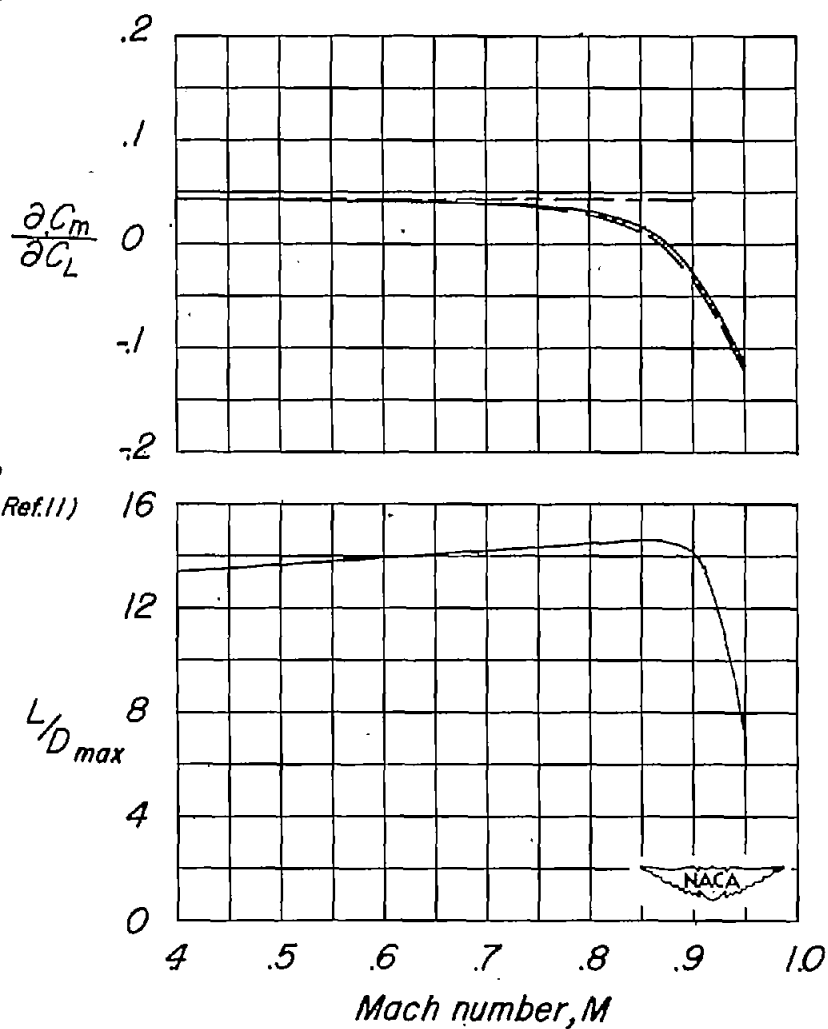
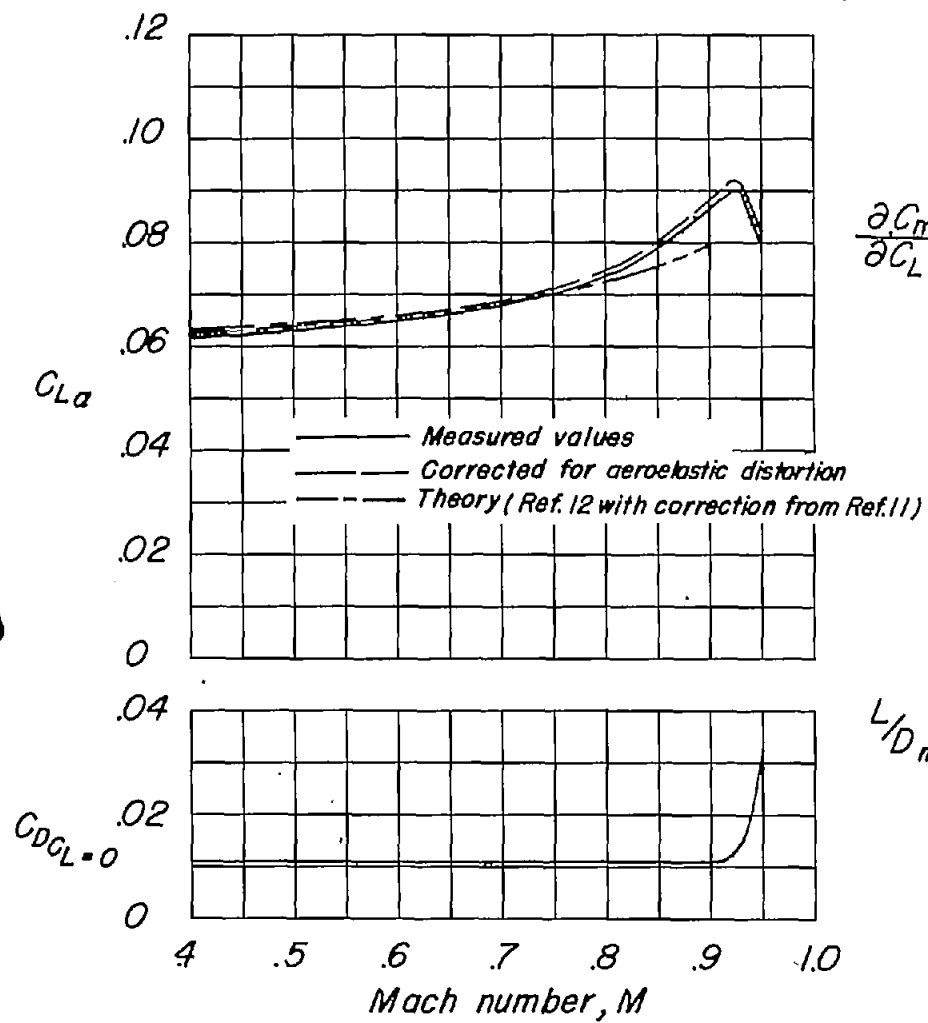


Figure 11.- Summary of the effect of Mach number on the aerodynamic characteristics of the 32.6-4-0.6-006 wing-fuselage combination.

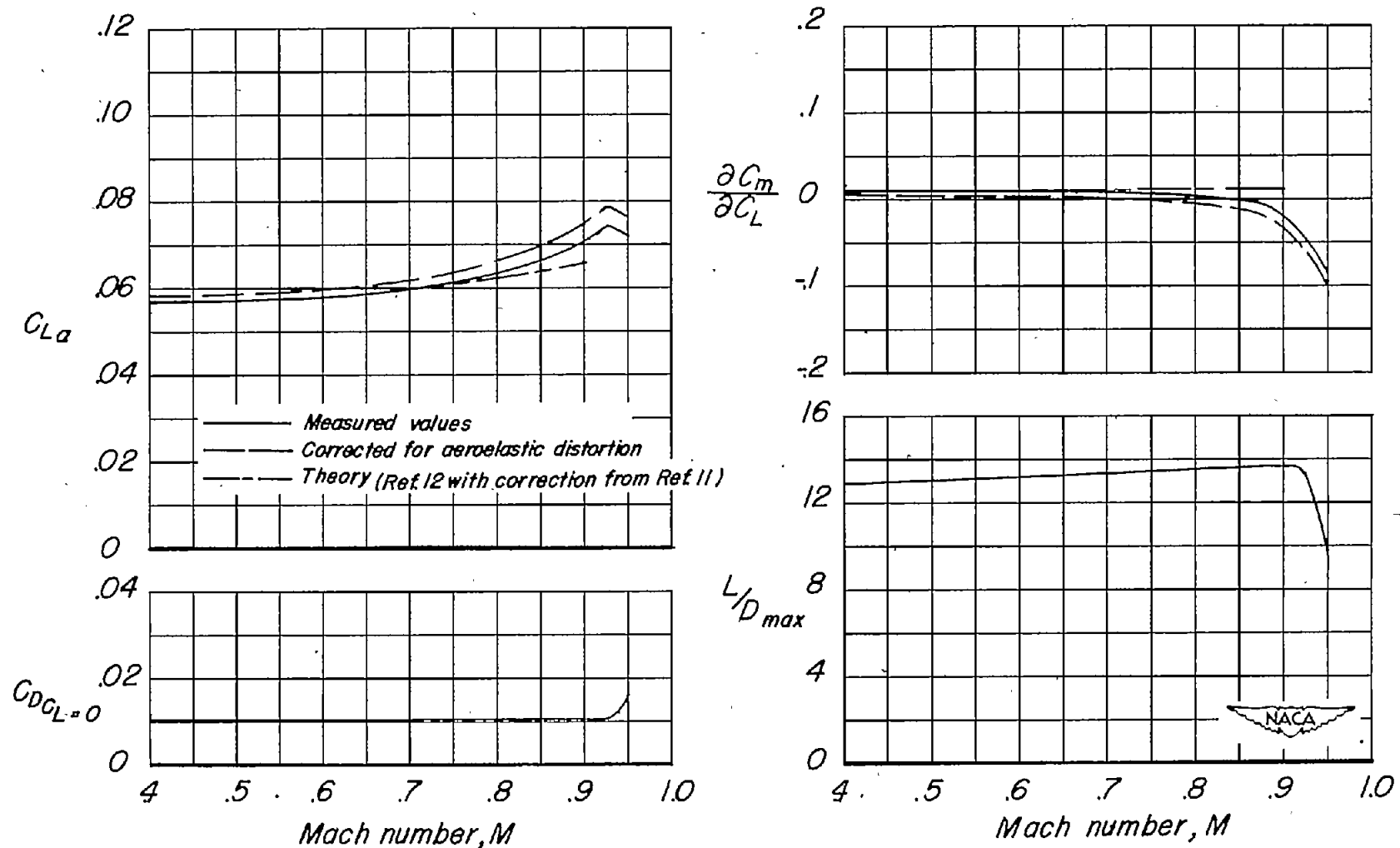


Figure 12.- Summary of the effect of Mach number on the aerodynamic characteristics of the 45-4-0.6-006 wing-fuselage combination.

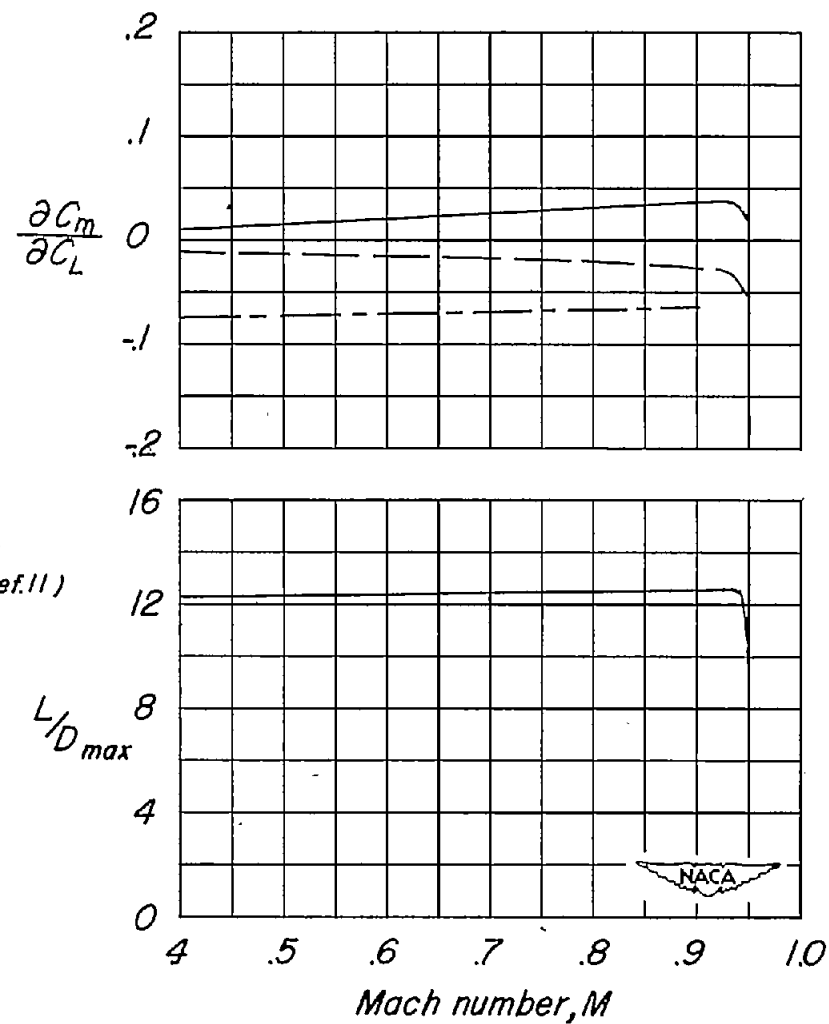
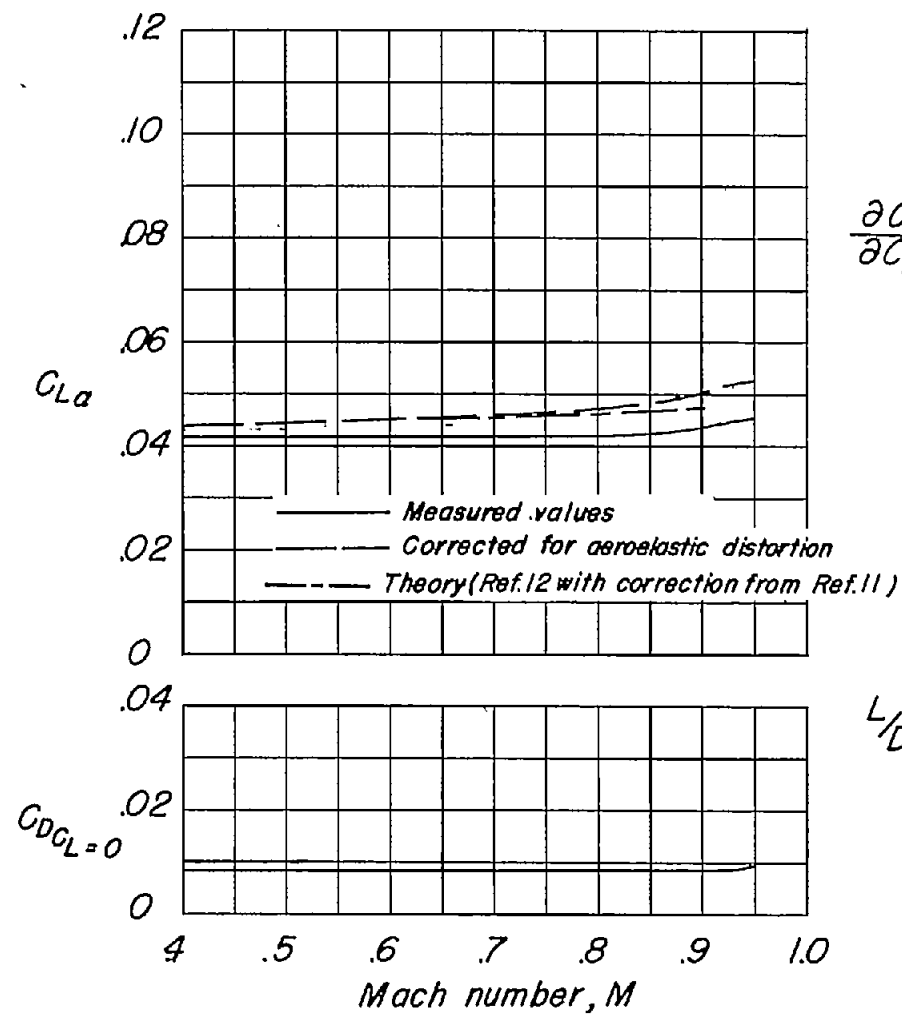


Figure 13.- Summary of the effect of Mach number on the aerodynamic characteristics of the 60-4-0.6-006 wing-fuselage combination.

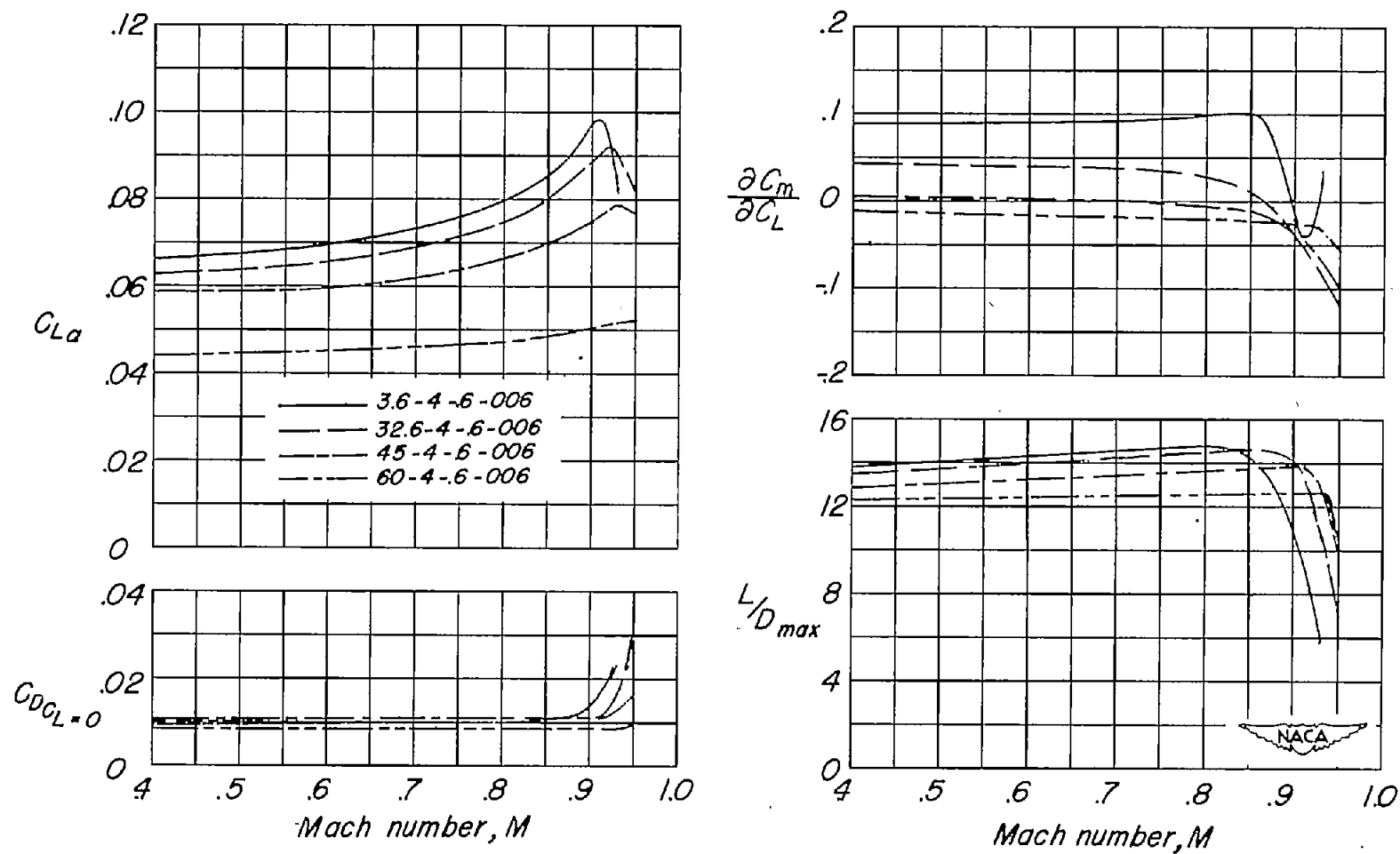


Figure 14.- Comparison of the effects of Mach number on the aerodynamic characteristics of the four wing-fuselage combinations. $\left(C_{L\alpha} \text{ and } \frac{\partial C_m}{\partial C_L} \right)$ corrected for aeroelastic distortion).

CONFIDENTIAL

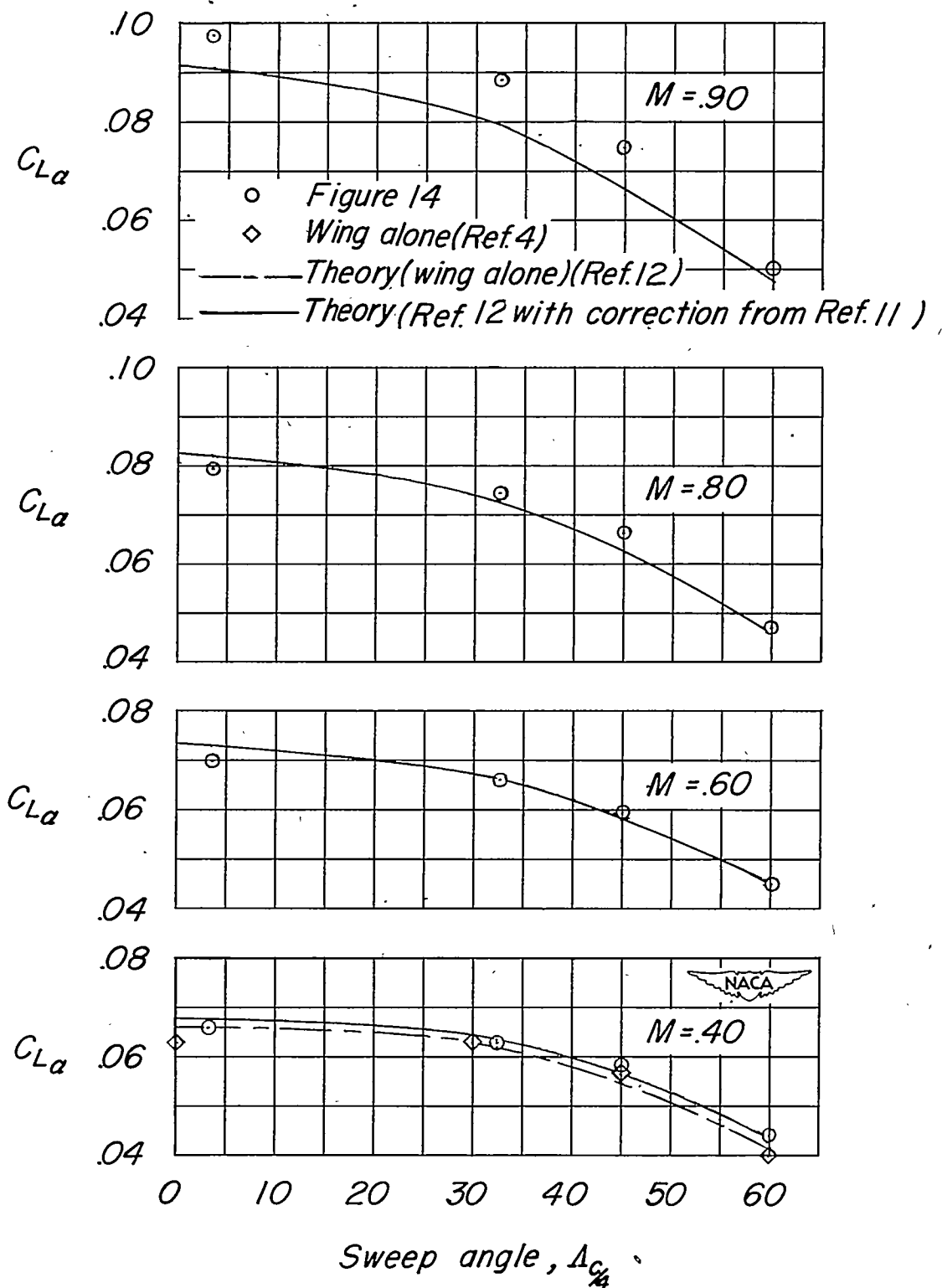


Figure 15.- Effect of sweep on the lift-curve slope at several Mach numbers. Corrected for aeroelastic distortion.

CONFIDENTIAL

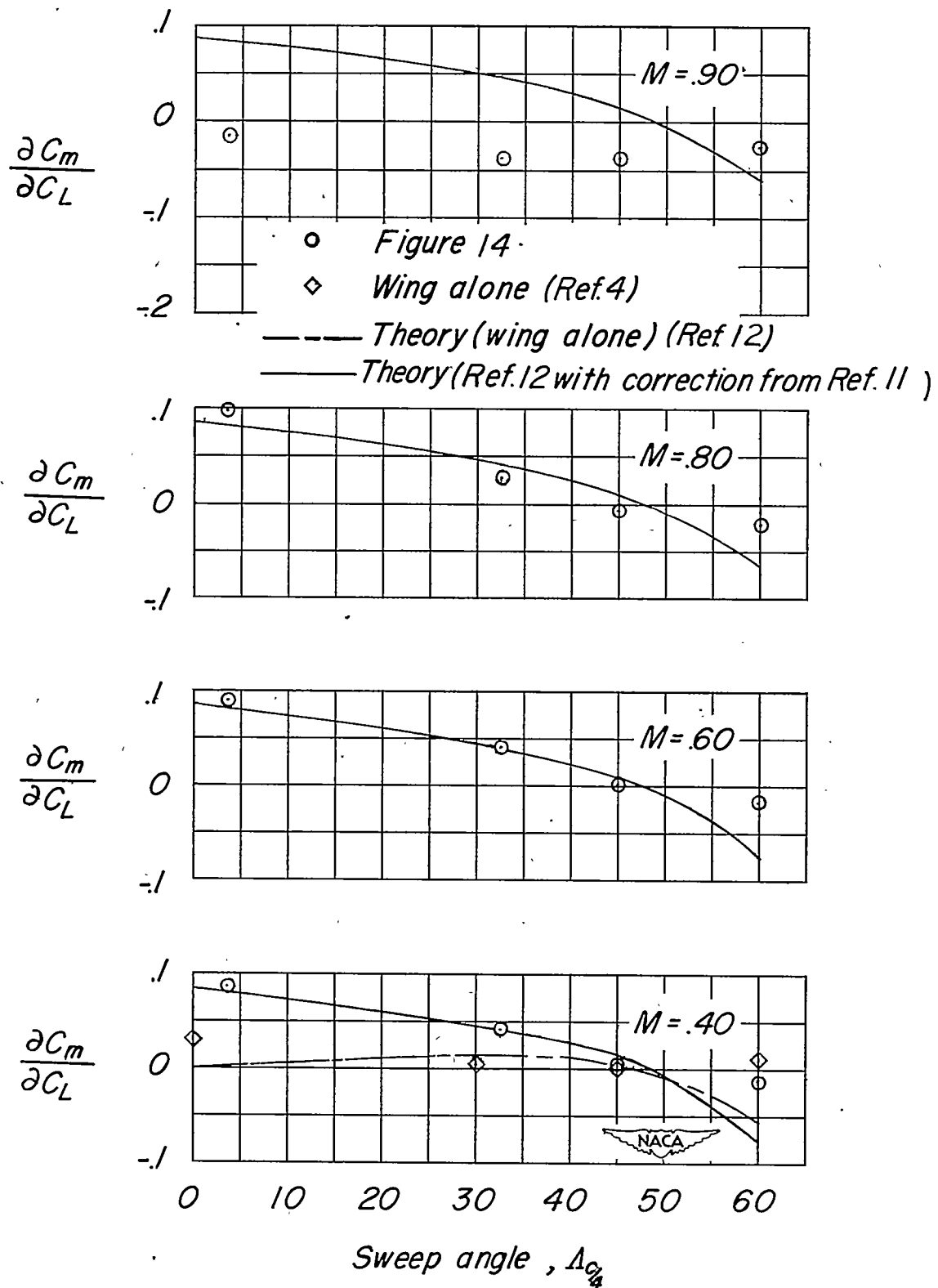


Figure 16.- Effect of sweep on the aerodynamic-center location at several Mach numbers. Corrected for aeroelastic distortion.

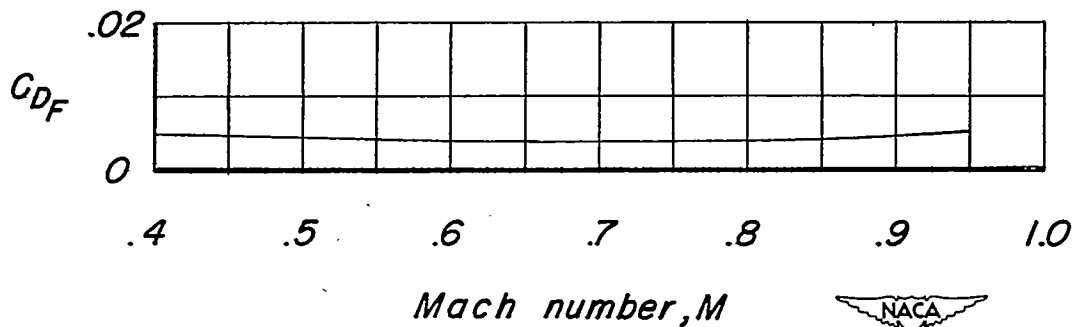


Figure 17.- Drag of the fuselage alone at zero angle of attack, based on the wing area.

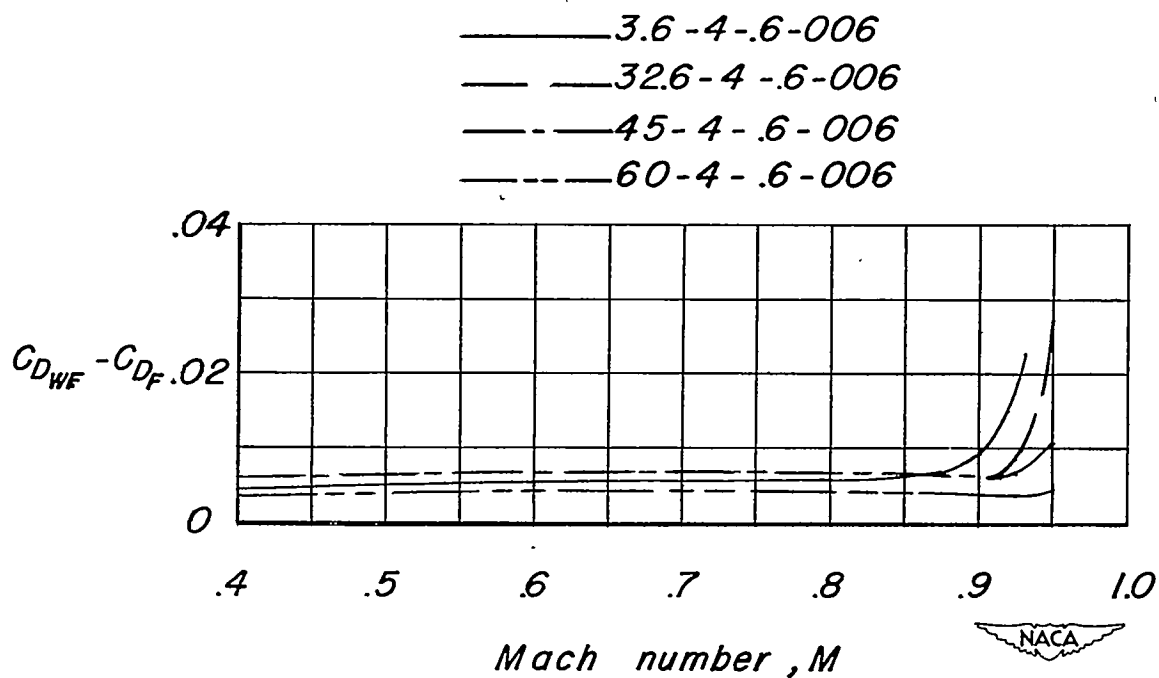


Figure 18.- Variation with Mach number of the wing plus wing-fuselage interference drag at zero lift for the four wings.

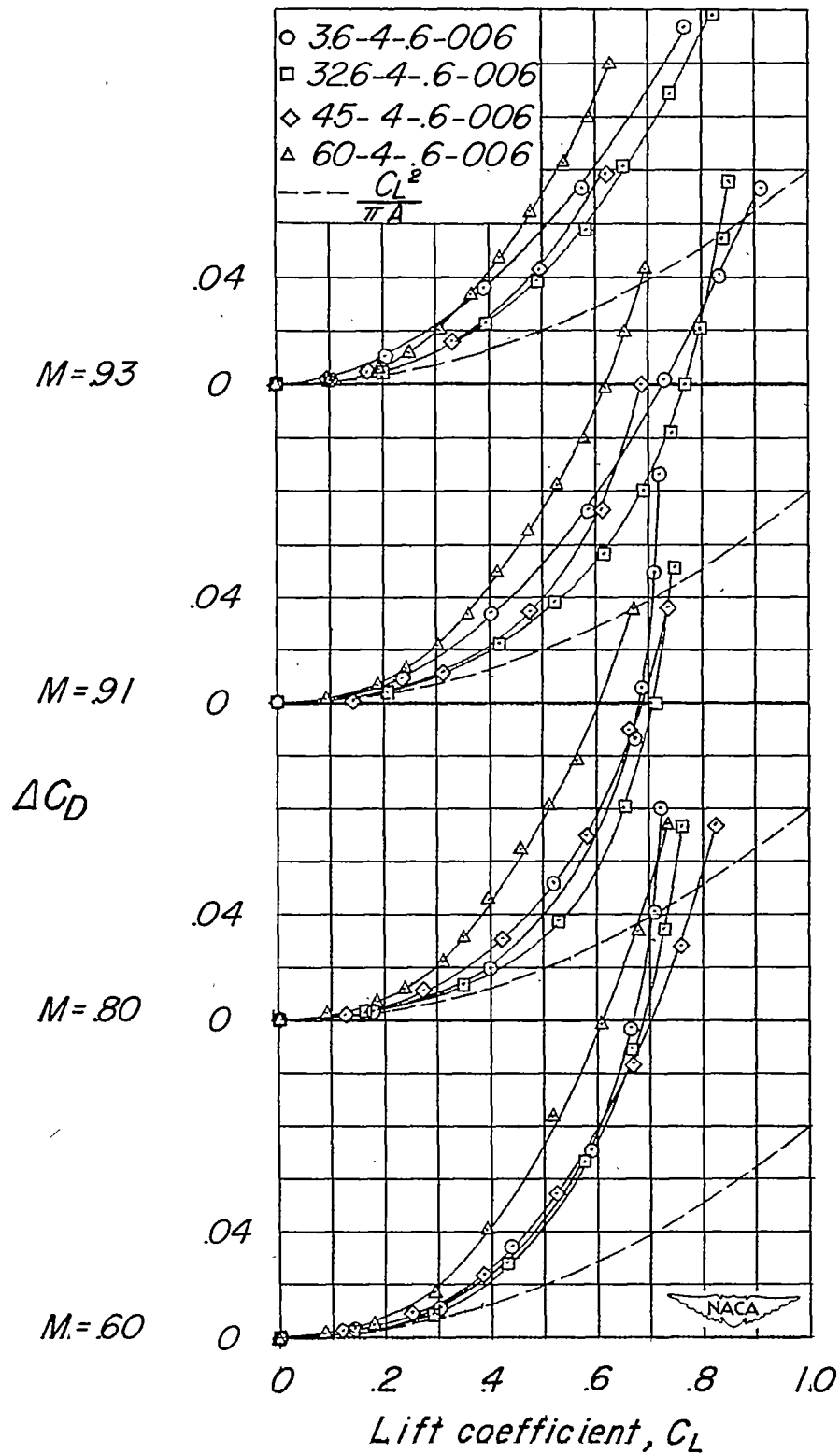


Figure 19.- Comparison of the effects of sweep angle on the drag due to lift at several Mach numbers.

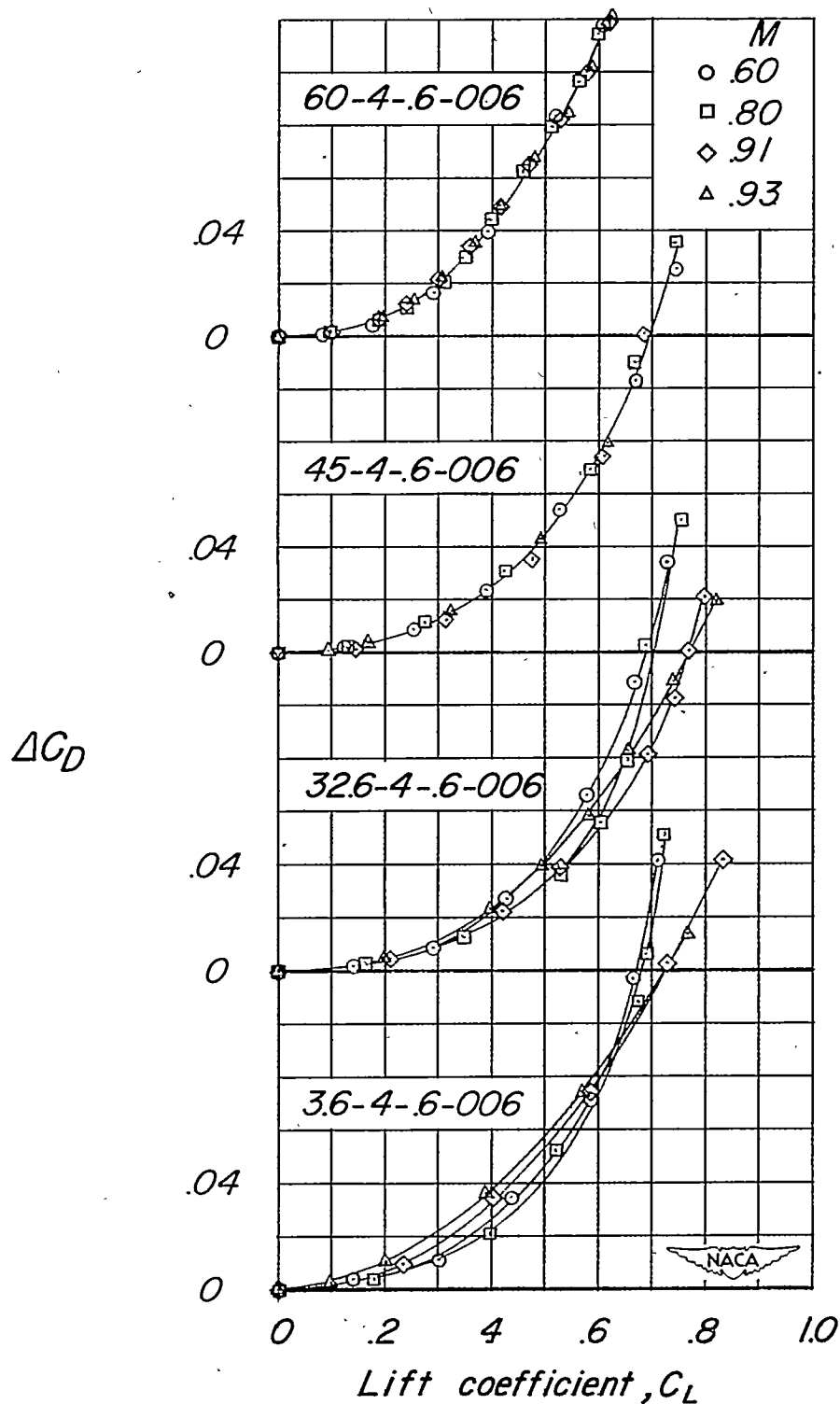


Figure 20.- Comparison of the effects of Mach number on the drag due to lift for the four wing-fuselage combinations.

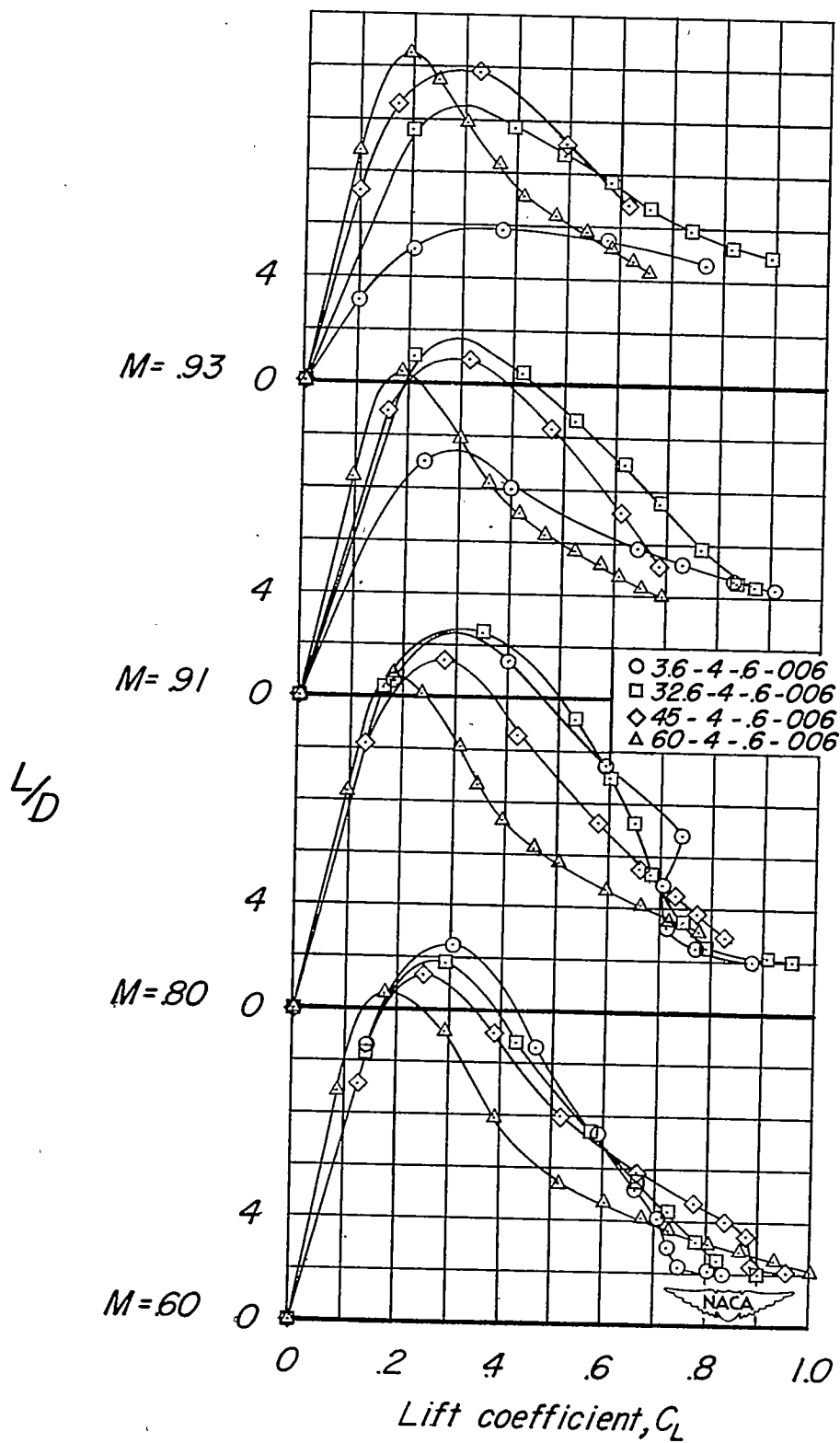


Figure 21.- Comparison of the lift-drag ratios of the four wing-fuselage combinations at several Mach numbers.